Magnetic recording, and phase transitions in the fcc Kagomé lattice:

A two-part talk.

Martin Plumer Memorial University of Newfoundland

Part I.
Ferromagnetism
(long-range dipole).

Part II.
Antiferromagnetism
(frustration).

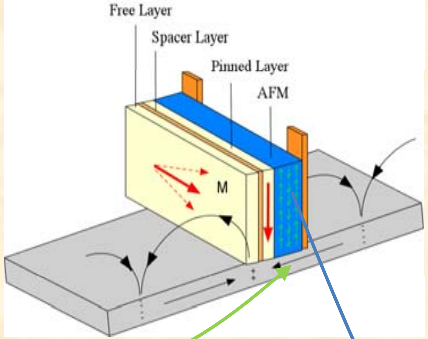

Exchange Pinning

$IrMn_3$

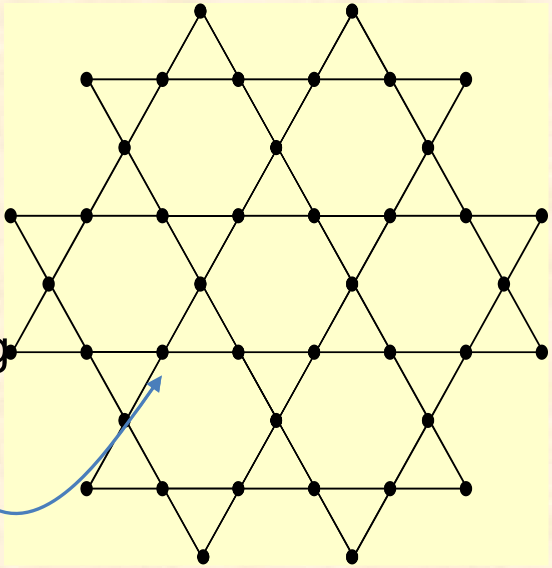

PART I. Review of Recent and Future Technologies in Magnetic Recording.

- Overview of *The Writer, The Reader* (Ir-Mn used for exchange pinning) and *The Media*.

- Areal Density Increase: ***The Superparamagnetic Trilemma.***

- Modeling with *micromagnetics* (LLG: Landau-Lifshitz-Gilbert equations).

- The Recent: Perpendicular Recording and Dual-Layer ECC media.

- The Future (?): Many-layer ECC media, HAMR and BPM.

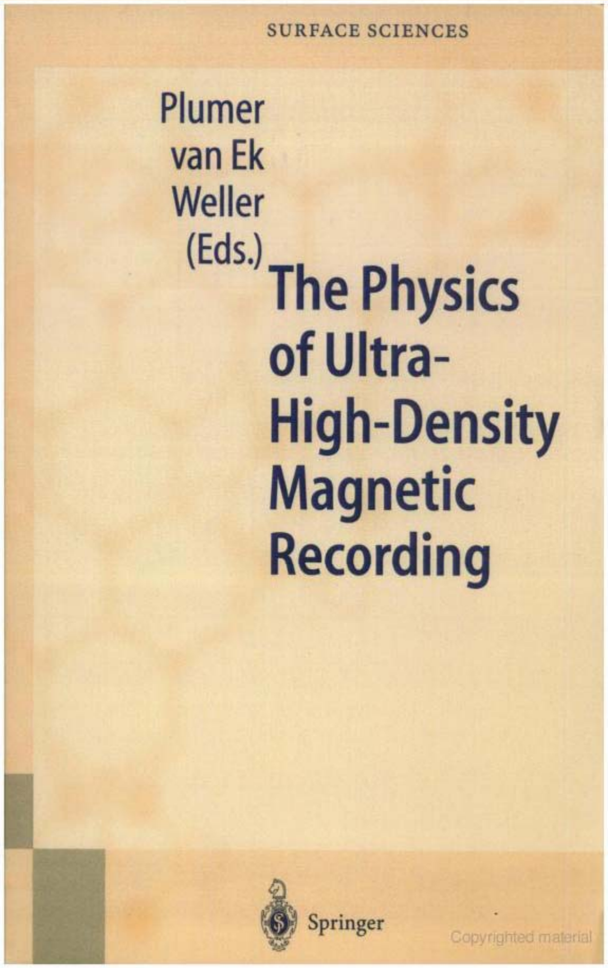

<u>PART II. Monte Carlo Simulations</u>

<u>*of ABC* stacked Kagomé planes</u>.

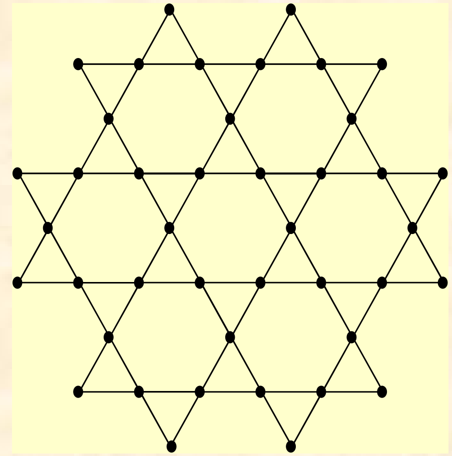

- Review of Exchange Pinning.
- $IrMn_3$ = fcc ABC stacked Kagomé lattice.
- XY and Heisenberg models with NN exchange (8 neighbors).
- Discontinuous transitions to LRO at finite T.
- Impact of spin degeneracies on sub-lattice order parameter.
- Anisotropy and future simulations of exchange bias.

Areal Density Growth

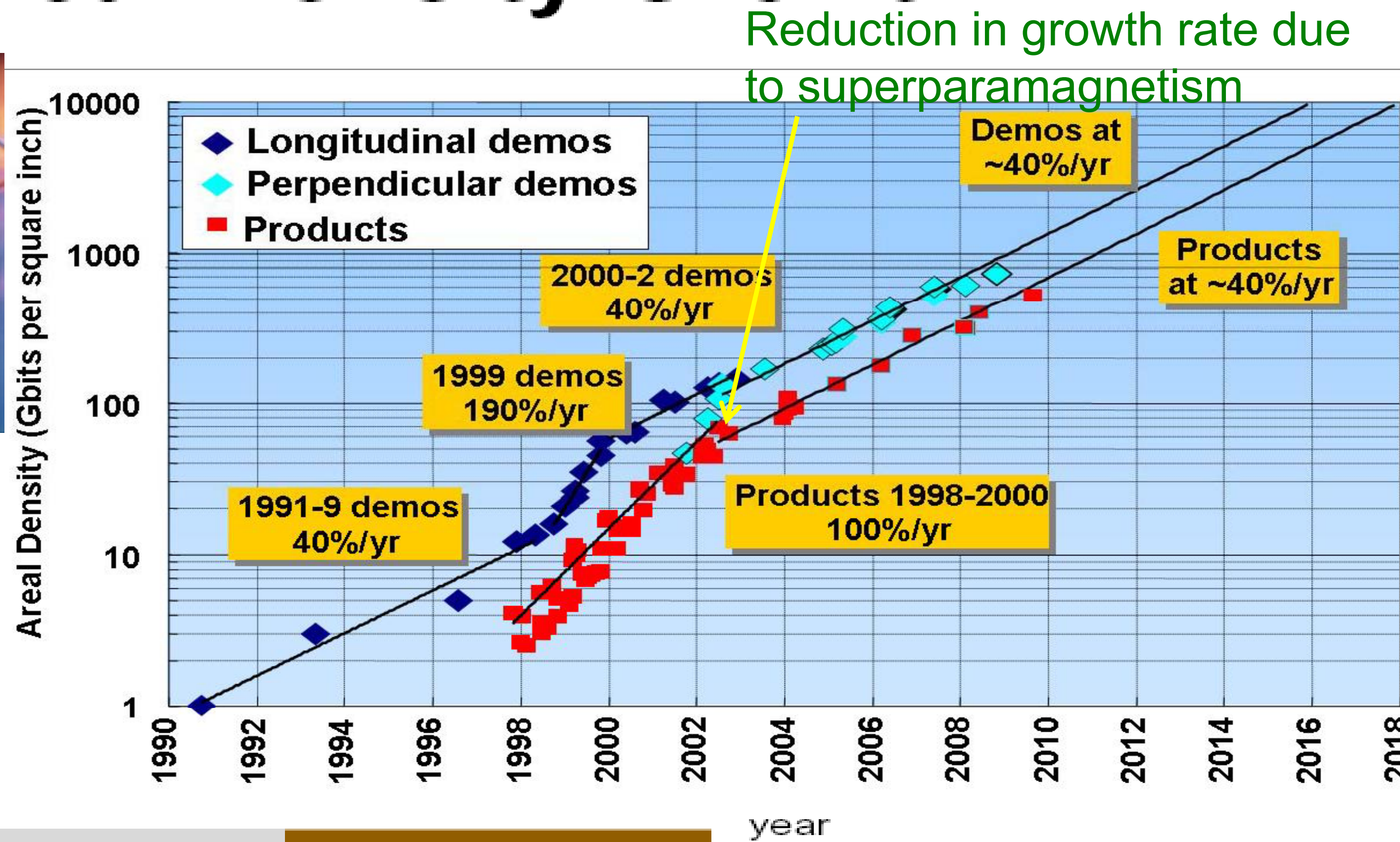

- Additional innovations required at that point
  - heat-assisted recording
  - bit patterned media recording

AD=(1/track width)*(1/bit length)
=(tracks per inch)(bits per inch)

- **Today: AD ~ 500Gb/in^2 Bit length ~ 2 media grains ~ 180 Å**
- **Tomorrow: AD ~ 1000Gb/in^2. Bit length ~ 1 media grain ~ 50 Å**

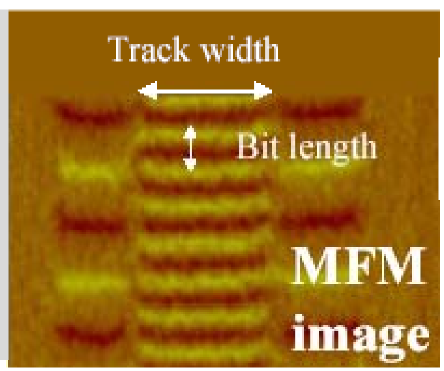

New Paradigms in Magnetic Recording, M.L. Plumer, J. van Ek, and W.C. Cain, Physics in Canada 67, 25 (2011)

The *three* elements of magnetic recording:
The Writer, The Reader, The Media.

Longitudinal Recording.

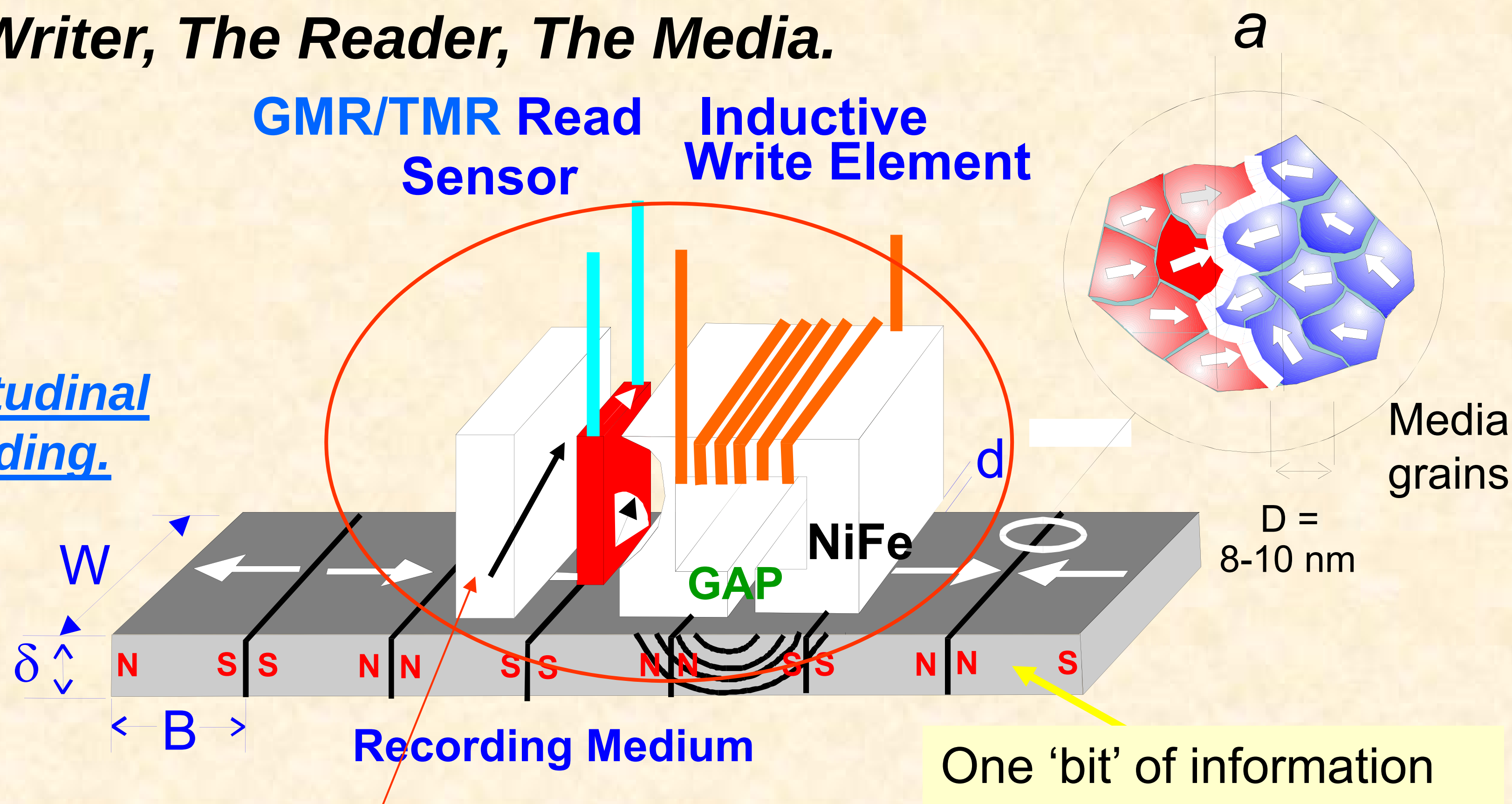

AD=(bpi)(tpi)
bpi ~ 1/B
tpi ~ 1/W

Recording Head

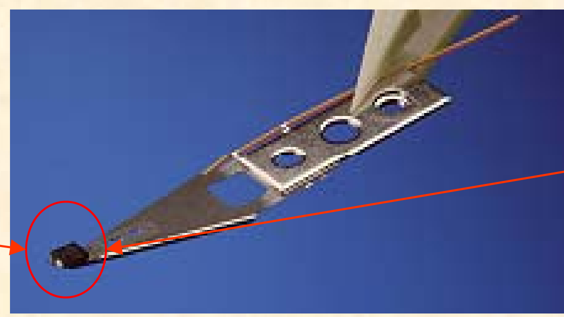

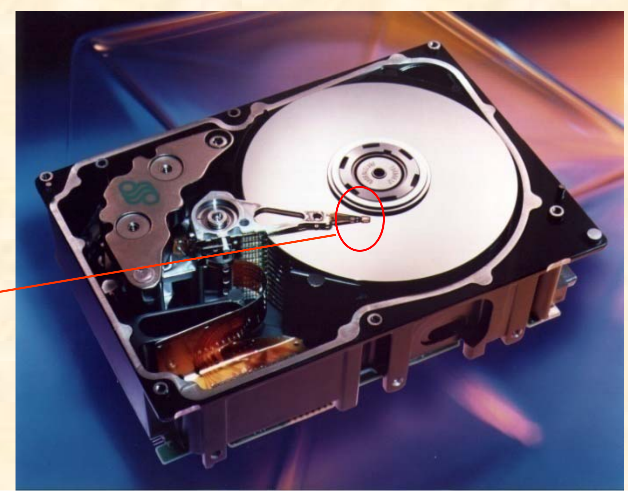

The HDD Head: Extreme Close-up

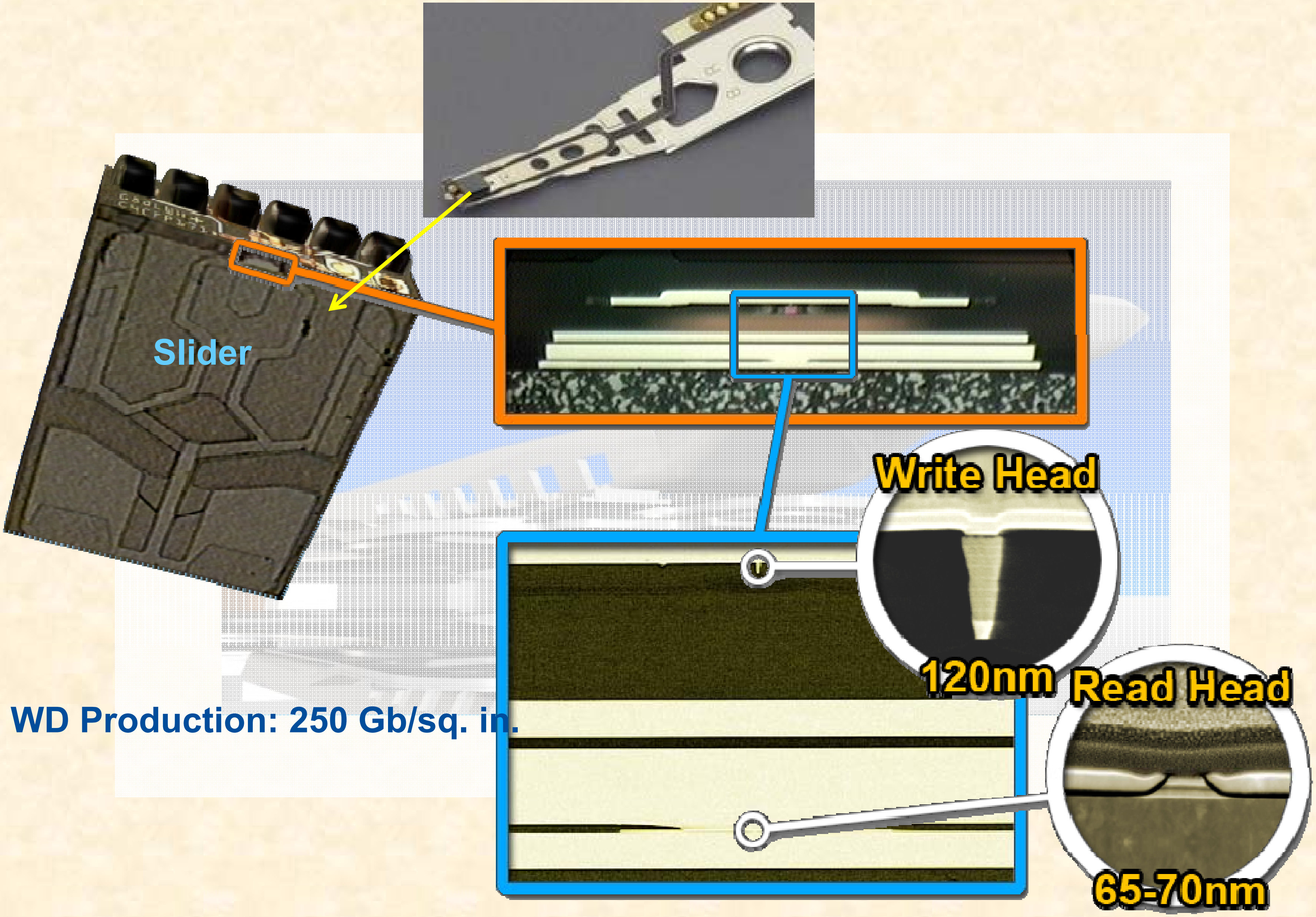

WD Production: 250 Gb/sq. in.

The Writer: Reversing the media magnetization

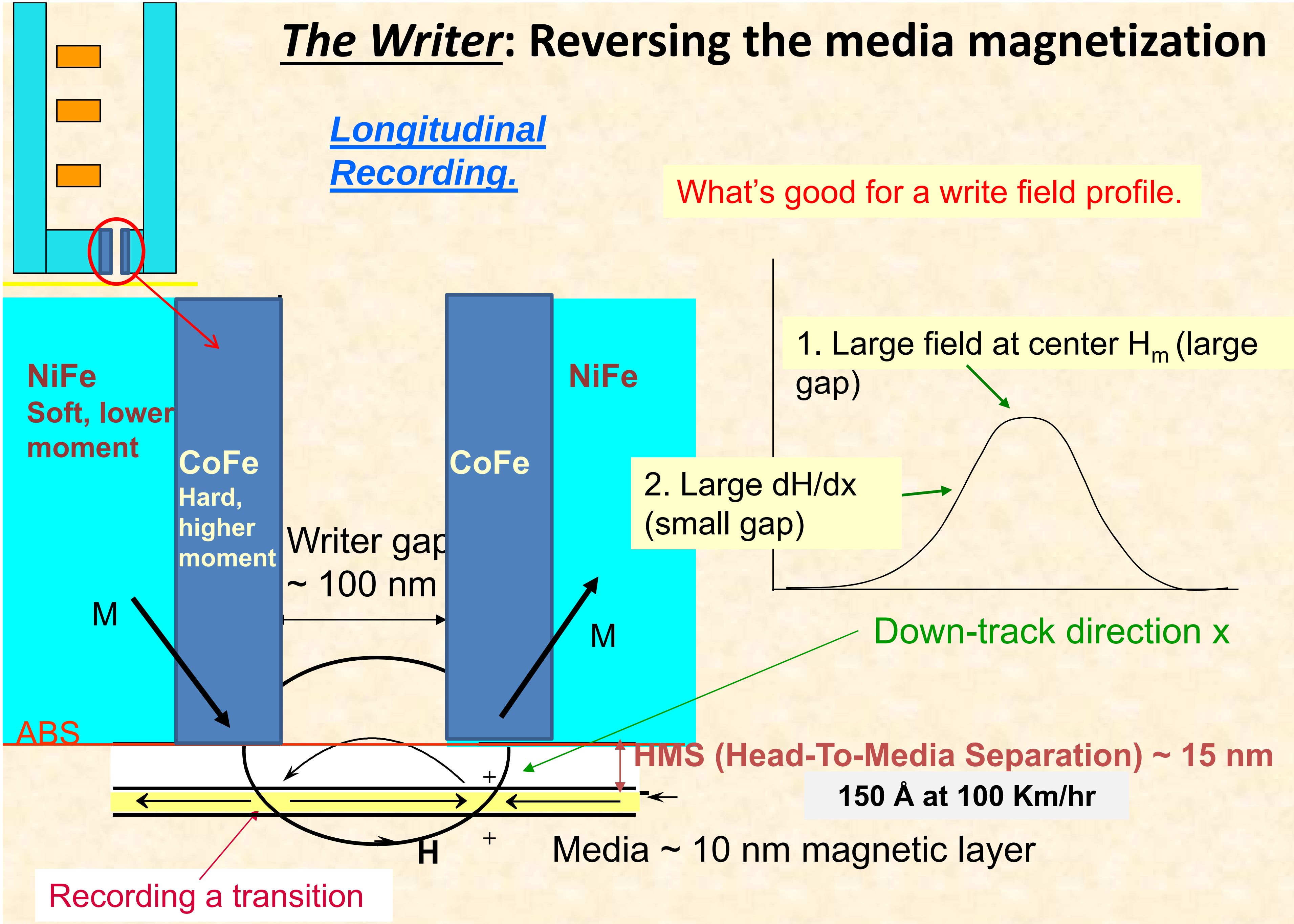

The Reader: Detection of media magnetization reversal.

GMR: 2007 Nobel Prize in Physics. Fert and Grünberg

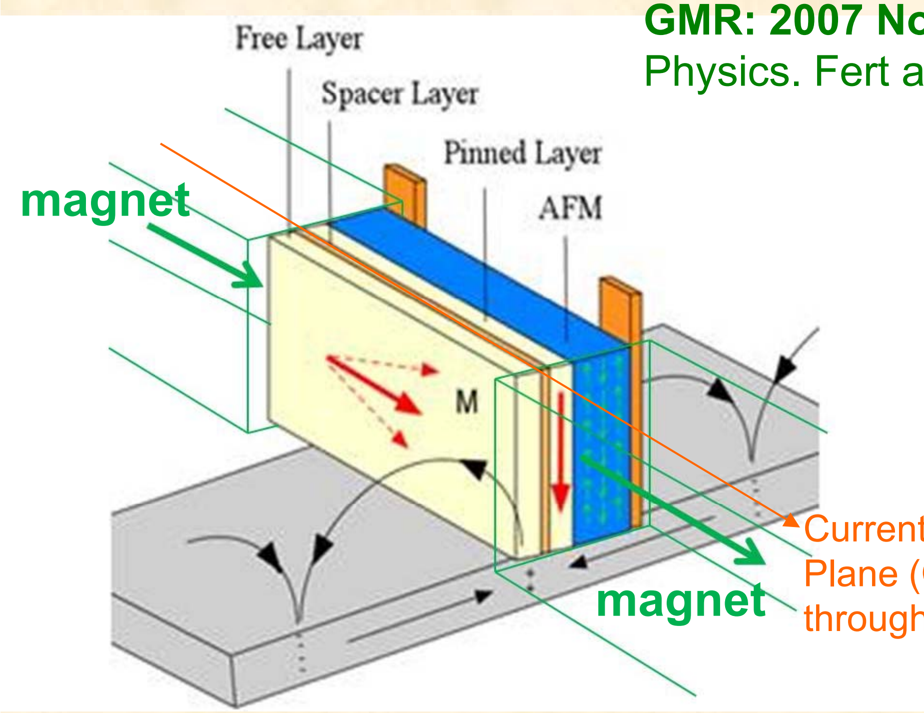

Current flows In the Plane (CIP), mainly through Cu layer.

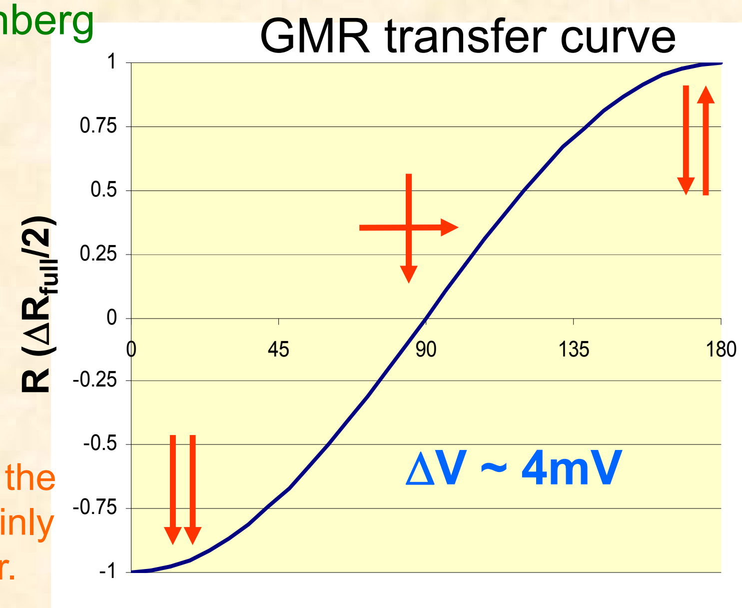

AFM = Ir-Mn (High T_N). 200 Å

media **PL = CoFe (big moment). 25 Å**

FL = $Ni_{80}Fe_{20}$ Permalloy 25 Å

TEM

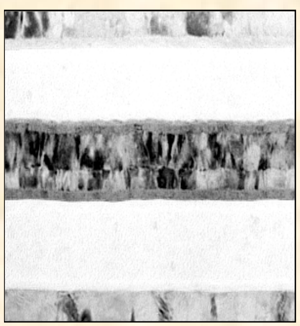

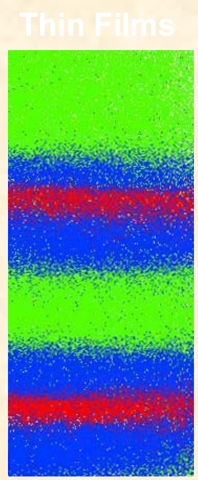

ABS view

GMR effect involves surface and bulk scattering of spin polarized electrons between the Free Layer and Pinned Layer.

The Media: A "hard" granular magnet

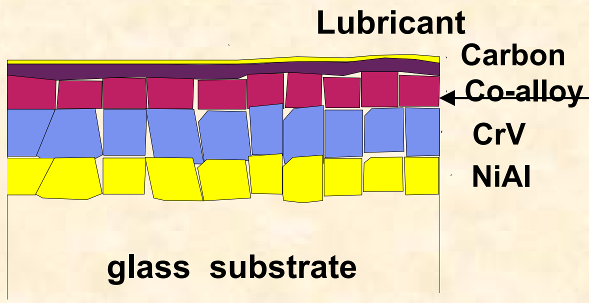

CoCrPt

longitudinal

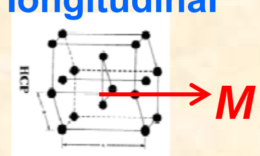

Need ΔE >> k_BT

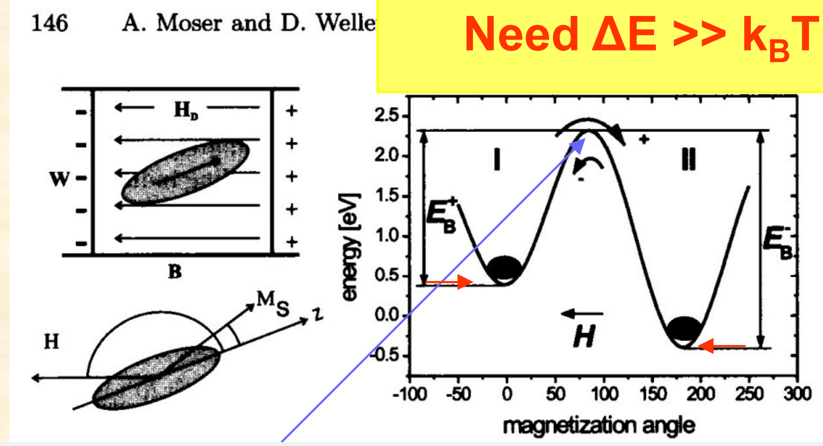

ΔE = (crystal anisotropy)(grain volume = K*V

Grain size ~ 16 nm

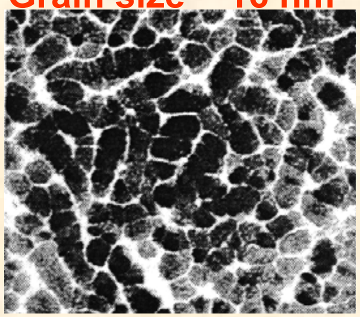

1 Gbit/in^2 media

Grain size ~ 9nm

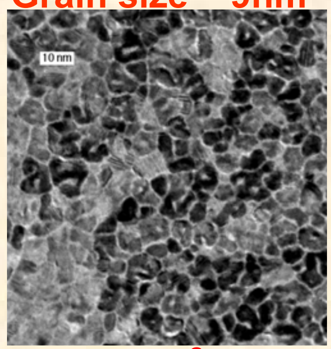

50 Gbit/in^2 media

Switching Field ~
Coercivity= H_c=2K/M_s

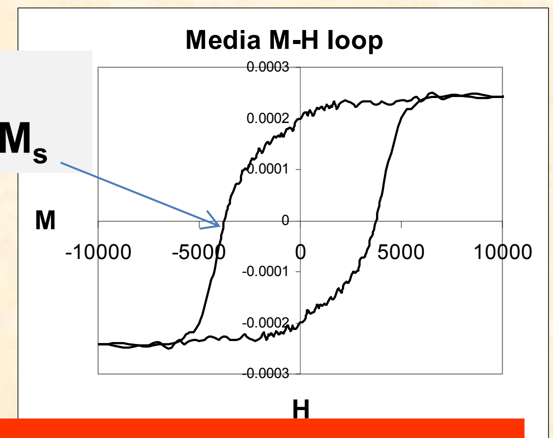

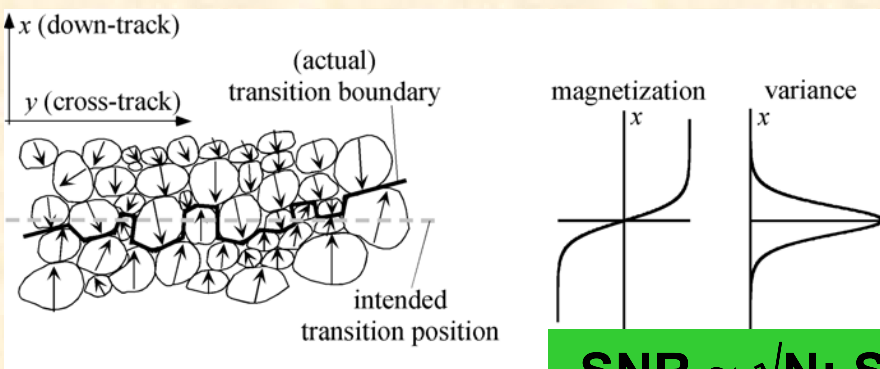

SUPERPARAMAGNETISM: Smaller grains are *worse* for thermal stability ('thermal idiots').

SNR ~ √N: Smaller grains are *better*.

The Trilemma of shrinking dimensions.

1. Smaller bits require smaller media grains to maintain SNR.
2. Smaller grains require larger anisotropy (energy barrier) to maintain thermal stability.
3. Larger anisotropy requires larger write fields to switch media transitions.

- Also: Smaller dimensions lead to less responsive read elements (magentically).
- Larger write fields require large moment materials to put at the business end of the write element.
- CoFe at 2.4 Tesla is the largest moment material stable at room temperature ***and has been used since 1999***.

Modeling to the rescue (and perpendicular recording and tunneling magnetoresistive read elements, …).

Modeling (Simulations) to the Rescue.

Micromagnetics of Ferromagnets: Interacting, ***uniformly magnetized grains.***

Thin ferromagnetic films with small shapes and big demagnetization (magnetostatic) fields at edges.

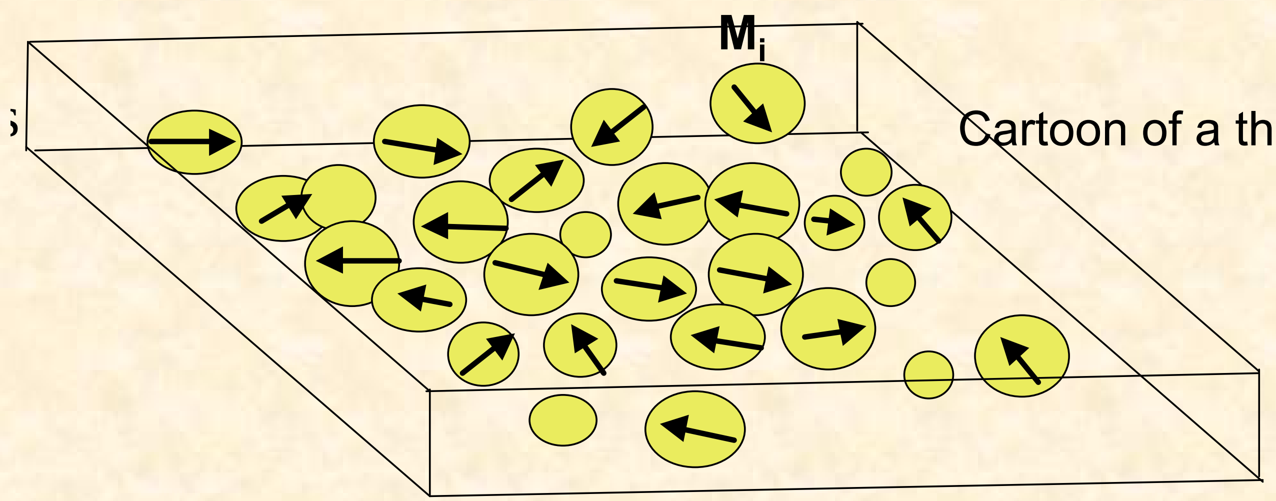

Cartoon of a thin film

Grain size ~ 8 nm ⇒ 1000's of atoms.

Landau-Lifschitz-Gilbert Equation

Precession and phenomenological damping:

Torque Equation

$$\frac{d\vec{M}}{dt} = -\gamma \vec{M} \times \vec{H}$$

Add damping

$$\vec{H}(\vec{r},t) \rightarrow \vec{H}_{\text{eff}}(\vec{r},t) - \eta \frac{d\vec{M}(\vec{r},t)}{dt}$$

LLG:

$$(1+\alpha^2)\frac{d\vec{M}}{dt} = -\gamma \vec{M} \times \vec{H}_{eff} - \frac{\alpha\gamma}{M}\vec{M} \times \left(\vec{M} \times \vec{H}_{eff}\right)$$

$\alpha = \eta\gamma M$

$$\vec{H}_{effective} = \vec{H}_{applied} + \vec{H}_{anisotropy} + \vec{H}_{exchange} + \vec{H}_{magnetostatic}$$

Not just dipole

Norm conserving:

$$\frac{d\left|\vec{M}\right|^2}{dt} = 2\vec{M} \cdot \frac{d\vec{M}}{dt} = 0$$

$$\vec{a} \cdot (\vec{a} \times \vec{b}) \equiv 0$$

$\alpha \sim 0.1 – 0.001$

Spin-wave interactions, magnetoelastic coupling, impurities,…

Shape Anisotropy: A simple argument

- Dipole-dipole interaction (first terms in multipole expansion of magnetostatic energy)

$$E = \sum_{\substack{pairs \\ ij}} \frac{\vec{m}_i \cdot \vec{m}_j}{r^3{}_{ij}} - \frac{3(\vec{m}_i \cdot \vec{r}_{ij})(\vec{m}_j \cdot \vec{r}_{ij})}{r^5{}_{ij}}$$

E=-**M•H**

- Consider energy of <u>dipole 1</u> (lattice spacing $a=r_{ij}$)

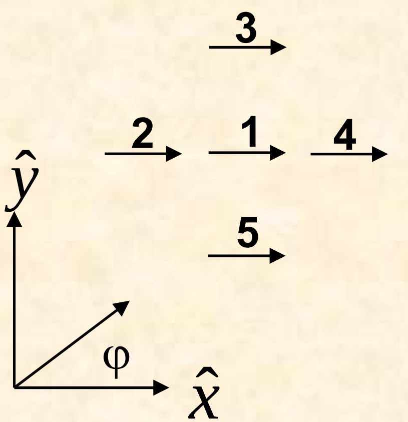

$$\frac{a^3 E}{m^2} = (\cos\phi_{12} + \cos\phi_{13} + \cos\phi_{14} + \cos\phi_{15})$$

$$-3(\cos\varphi_1 \cos\varphi_2 + \cos\varphi_1 \cos\varphi_4 + \sin\varphi_1 \sin\varphi_3 + \sin\varphi_1 \sin\varphi_5)$$

Put $\phi_i \equiv \phi$

$$= 4 - 3(2\cos^2\varphi + 2\sin^2\varphi) = -2$$

Completely isotropic.

Shape Anisotropy: A simple argument

- Create edge (remove 3)

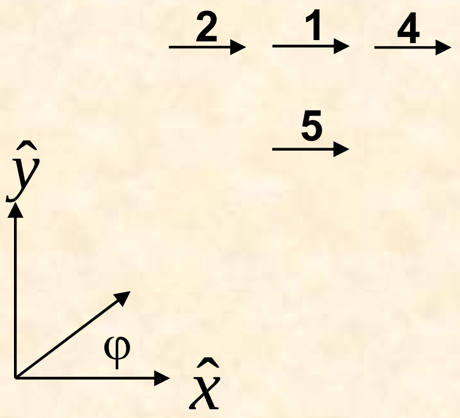

$$\frac{a^3 E}{m^2} = (\cos\phi_{12} + \cos\phi_{14} + \cos\phi_{15})$$
$$-3(\cos\varphi_1 \cos\varphi_2 + \cos\varphi_1 \cos\varphi_4 + \sin\varphi_1 \sin\varphi_5)$$

Put $\phi_i \equiv \phi$

$$= 3 - 3(2\cos^2\varphi + \sin^2\varphi) = 3 - 3\cos^2\varphi = 3\sin^2\varphi$$

Uni-axial anisotropy induced by edge. Energetically favorable for spins to align parallel to the edge and to neighboring spins.

Patterned Devices: Shape Anisotropy

- Series of solutions for platelets with different aspect ratios: What do we see?
  - CoFe, 2.5 nm thick, 10 nm cells (single layer)

Micromagnetic Modeling

Steady State Solution

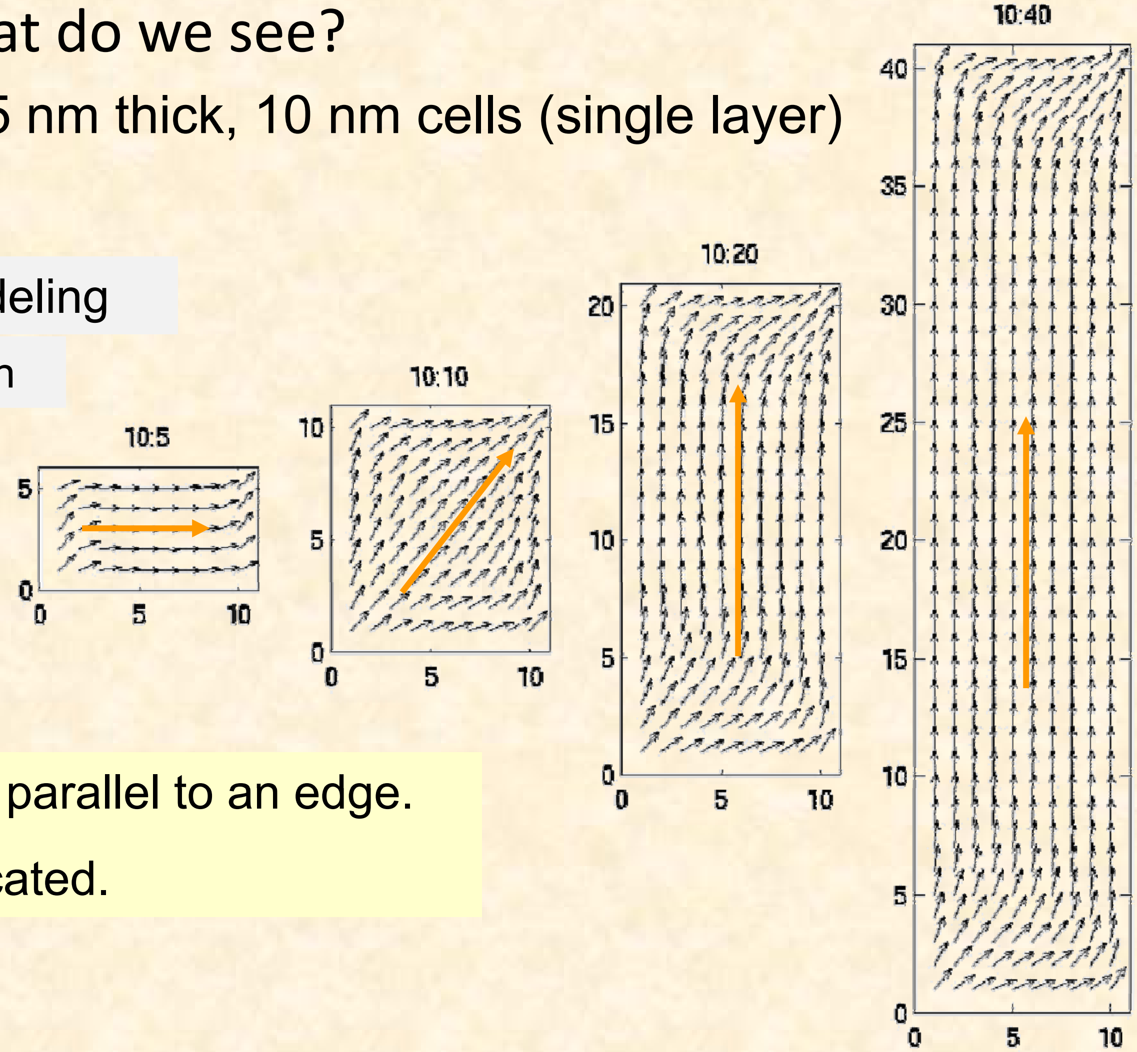

•Moments tend to lie parallel to an edge.

•Corners are complicated.

GMR spin valve response to a media transition field.

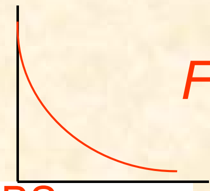

Field from media transition decays quickly

Quiescent state (H=0)

Response to field from a media

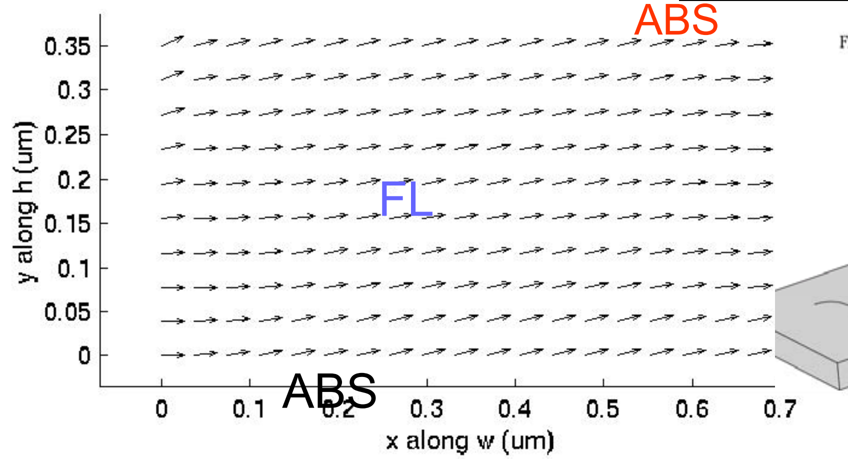

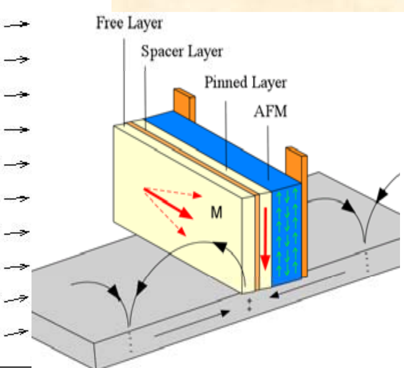

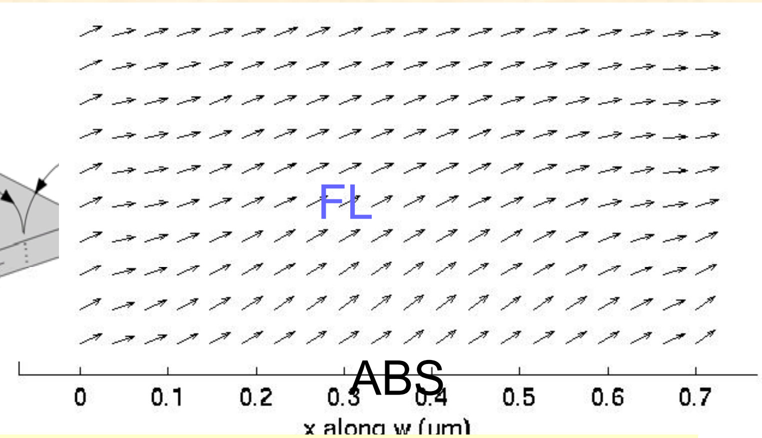

Shape anisotropy limits response for smaller devices.

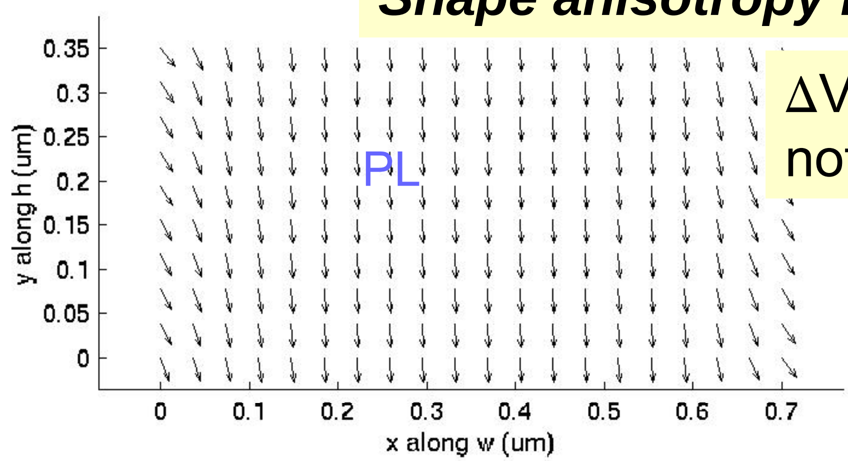

ΔV=1mV, not 4mV.

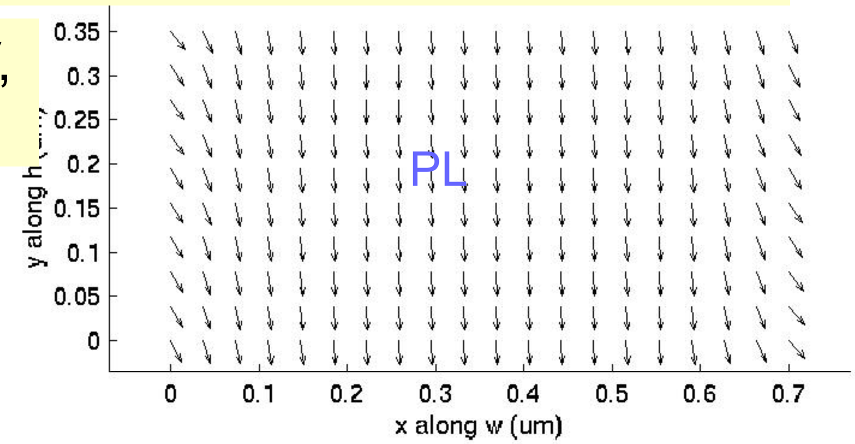

Micromagnetics of Medium Orientation Effects

Orientation Ratio (OR) accounted for by assuming a Gaussian distribution for the media *grain anisotropy axes direction* $\mathbf{H_K}$: mean and Standard Deviation.

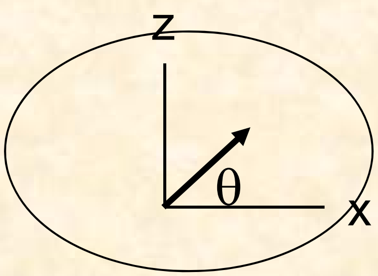

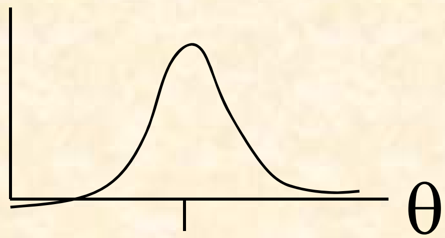

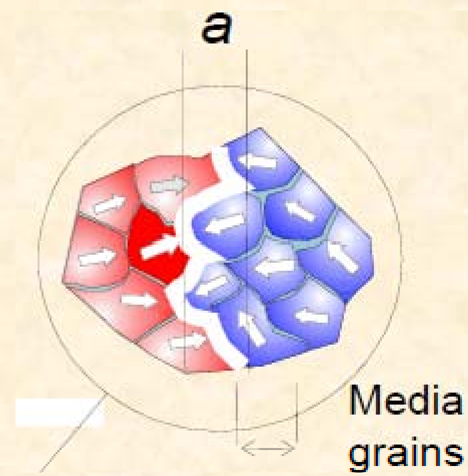

Isotropic media – very large standard deviation.

Oriented media – smaller standard deviation (SD).

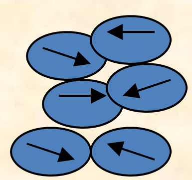

Expect better performance for media with a preference for **M** to lie in the down-track direction.

$100Gb/in^2$. Recorded tracks at high kbpi much improved with oriented media.

Isotropic media.

290 and 640 kbpi.

Oriented media.

640 kbpi.

OR ~ 1/SD

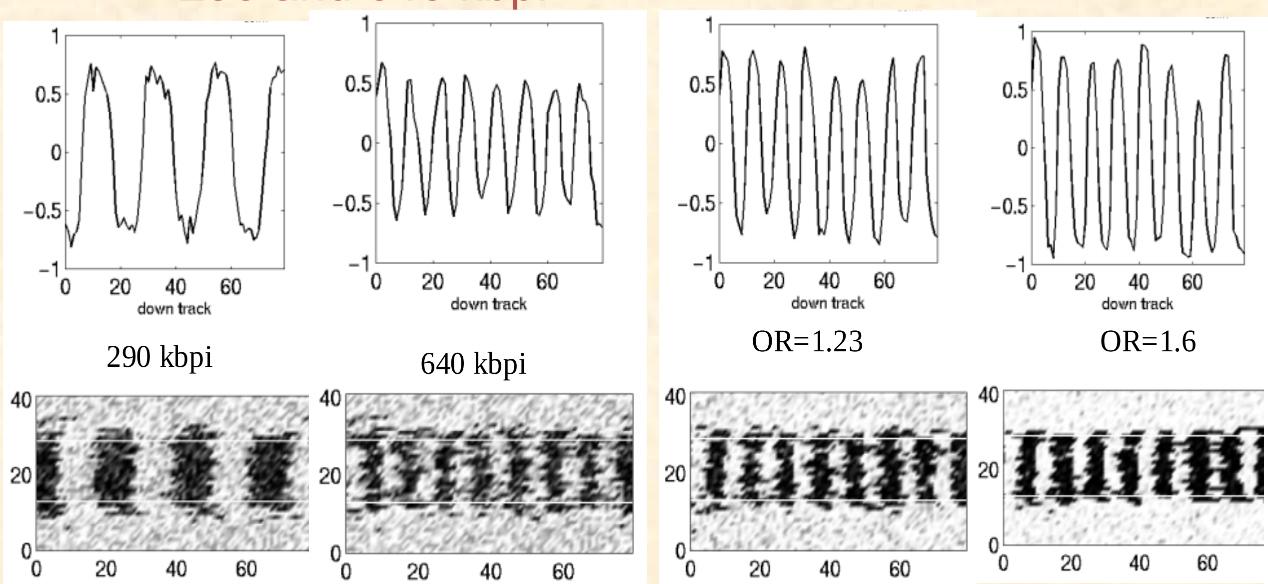

Amplitude vs OR

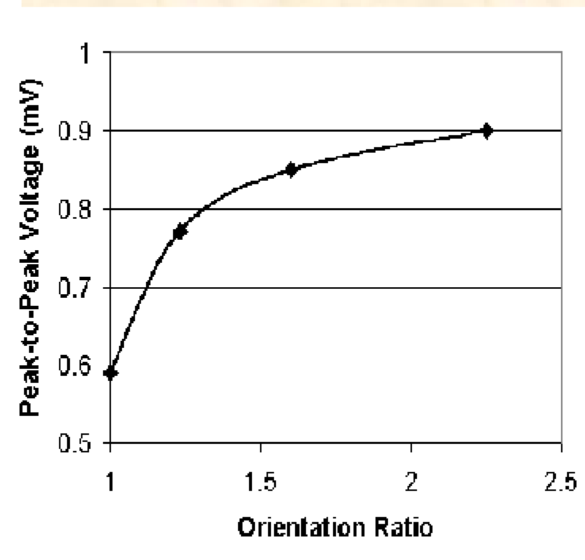

A clear message was received by recording media development groups. Highly oriented media became the industry standard.

What then ? *Perpendicular Recording* (even more ‘oriented’)

From *Yahoo.com Jan. 16, 2006.*

Technology Boosts Hard Drive Capacity (120 GB to 160 GB)

By MATTHEW FORDAHL, AP Technology Writer 1 hour, 8 minutes ago

SAN JOSE, Calif. - **Seagate Technology LLC has started shipping a notebook PC hard drive that overcomes an obstacle many feared would be a major roadblock to the further expansion of disk capacity — and the overall growth of the storage industry.**

The new approach that aligns bits of data vertically rather than horizontally enables Seagate — and other drive vendors — to further boost the density of drives without increasing the risk of scrambling data.

Perpendicular Recording: The ultimate in control of anisotropy-direction distributions

Longitudinal Recording

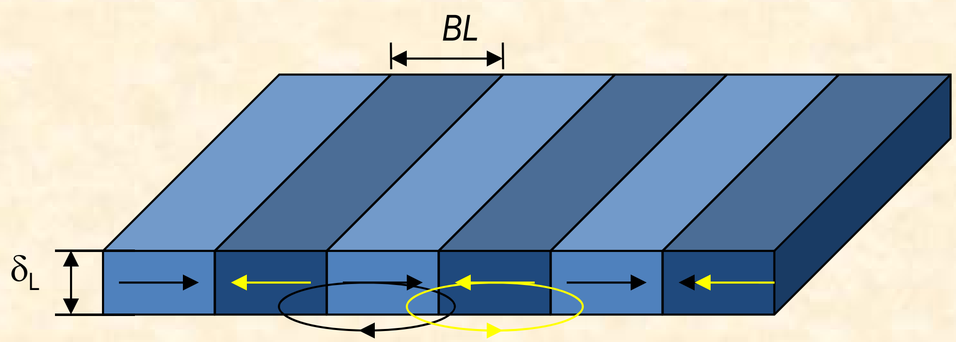

Magnetostatic fields destabilize the transitions (superparamagnetism).

Perpendicular Recording

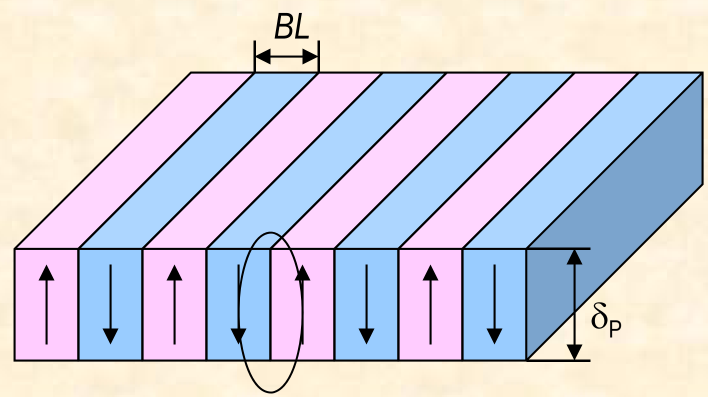

Magnetostatic fields stabilize the transitions.

Cobalt

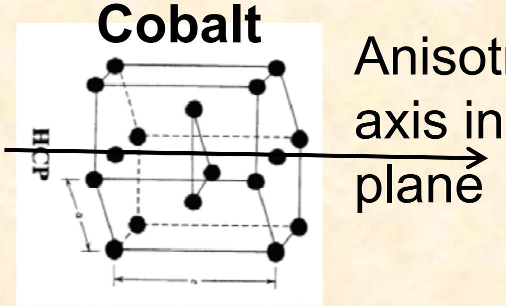

Anisotropy axis in plane

Hard to control distributions

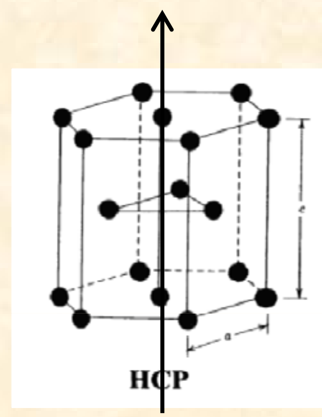

Anisotropy axis out of plane

Easier to control

Larger Write Fields due to media soft underlayer.

<u>Longitudinal Recording</u>

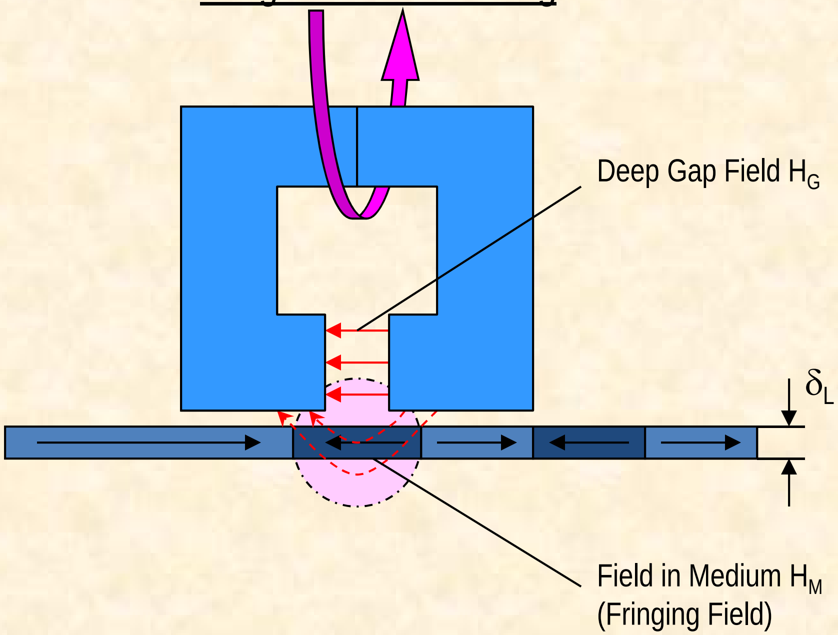

Single layer medium (longitudinal or perpendicular):

- *Transition is recorded by fringing field*

<u>Perpendicular Recording</u>

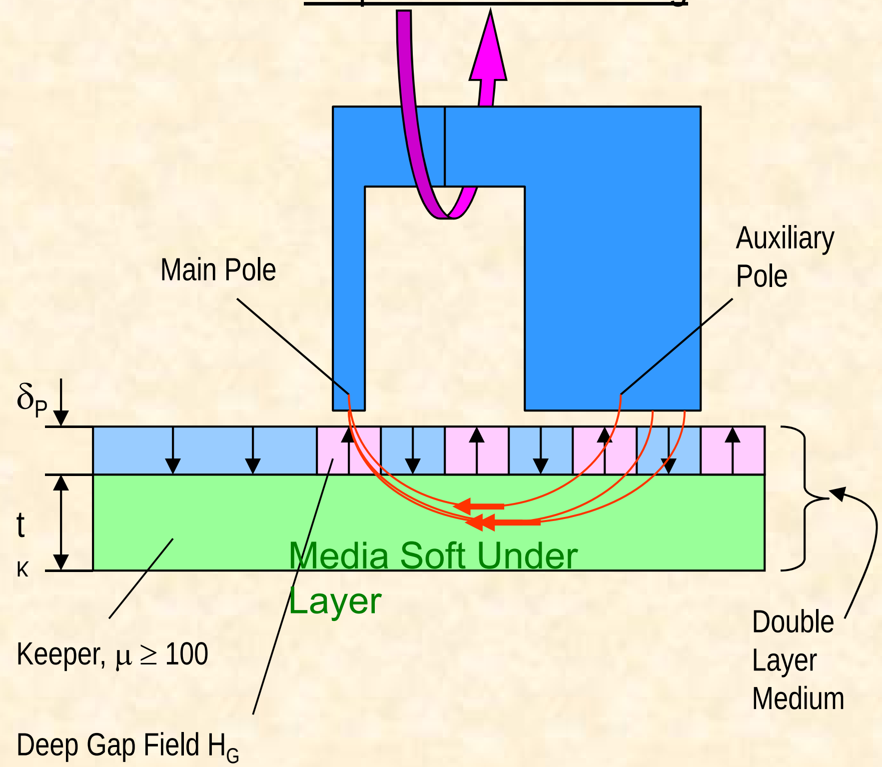

Double layer perpendicular media with soft magnetic Underlayer: media becomes part of the write element

- *Transition is recorded by deep gap field: 50 % boost.*

…and more field emanating from media transitions

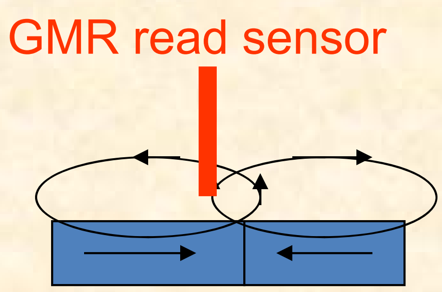

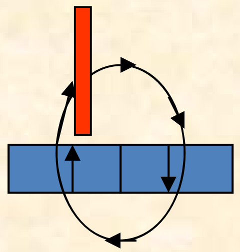

Stronger fields from perpendicular bits = larger play-back amplitude.

Another ~50% boost.

And TMR…Tunneling GMR Heads:

Double the read-sensor amplitude.

- **New Structure**
- **New materials**
- **New physics**

(aka: MTJ, SDJ,Tunnel valve, spin tunneling head)

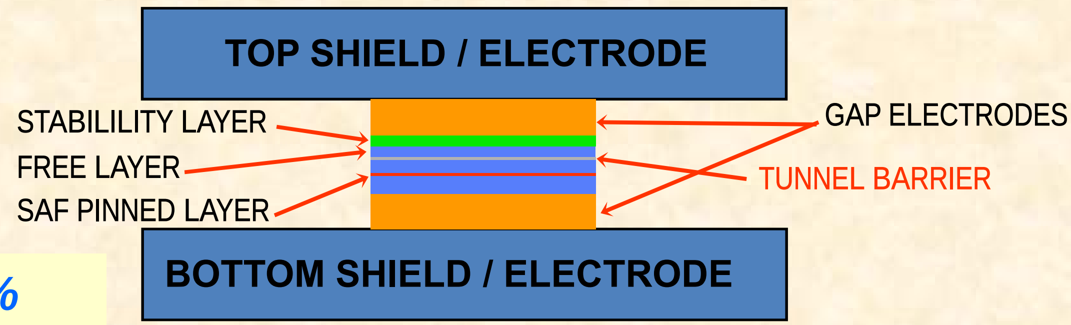

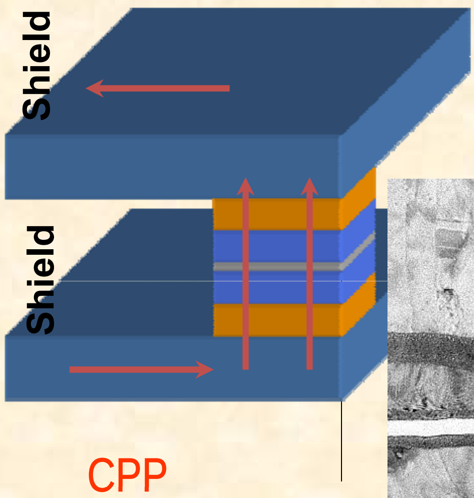

Another 50% boost in amplitude.

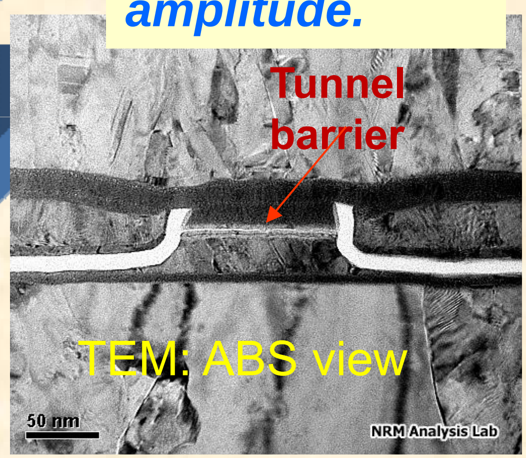

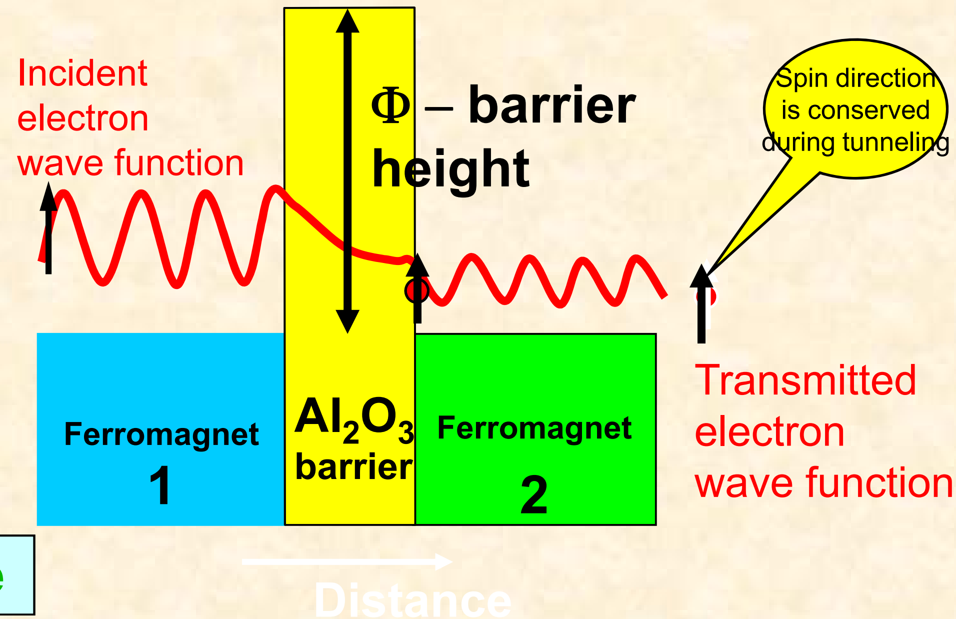

CPP = Current Perpendicular to Plane

Still requires exchange pinning of PL.

Exchange-Coupled-Composite Media:

Easier to reverse with same thermal stability.

Gerardo **BERTERO** Western Digital Corporation

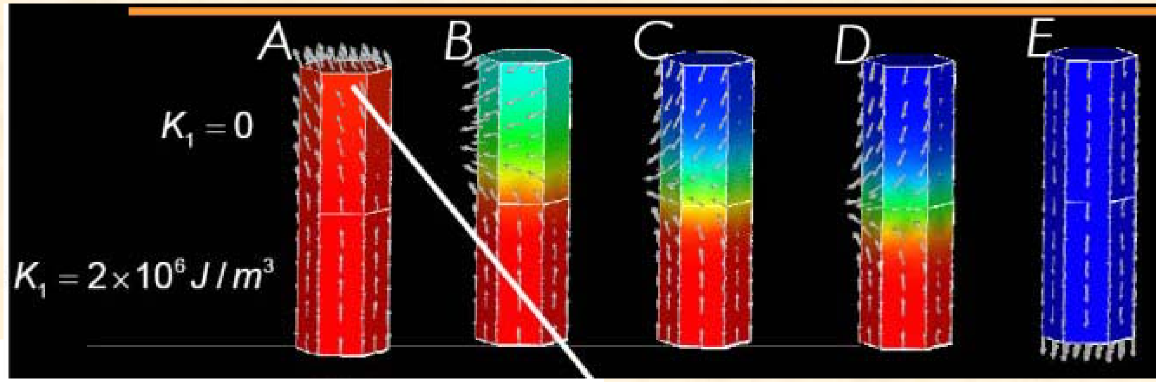

Introduction to ECC media

Material with extremely high anisotropy Ku and volume V_{hard}. Store information. Provide thermal stability

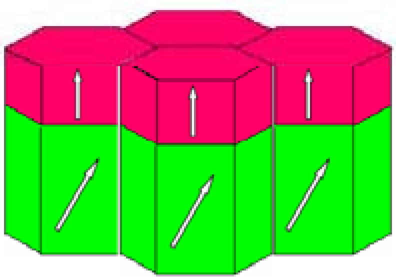

Soft material with volume V_{soft}. Facilitate switching of the grain.

$$\xi = \frac{2\Delta E}{M_s H_s V}$$

ΔE: $K_u x V_{hard}$

V: $V_{hard} + V_{soft}$

M_s: $\frac{(M_{hard}V_{hard} + M_{soft}V_{soft})}{V_{hard} + V_{soft}}$

This term can be used to compare the switching fields of different kind of media with the same thermal barrier, volume and magnetization

UNIVERSITY OF MINNESOTA

R.H. Victora and X. Shen, *IEEE Magnetics* ***41,*** *537-542 (2005).*

D. Suess *et al., J. Magn. Magn. Mat.* ***551,*** *290-291 (2005).*

Figure of merit:

Ratio of thermal energy barrier to switching energy.

ξ = 1 for single-layer

ξ = 2 for dual-layer

Now What ?

Try more: Multi-Layer ECC Media

Gerardo BERTERO Western Digital Corporation

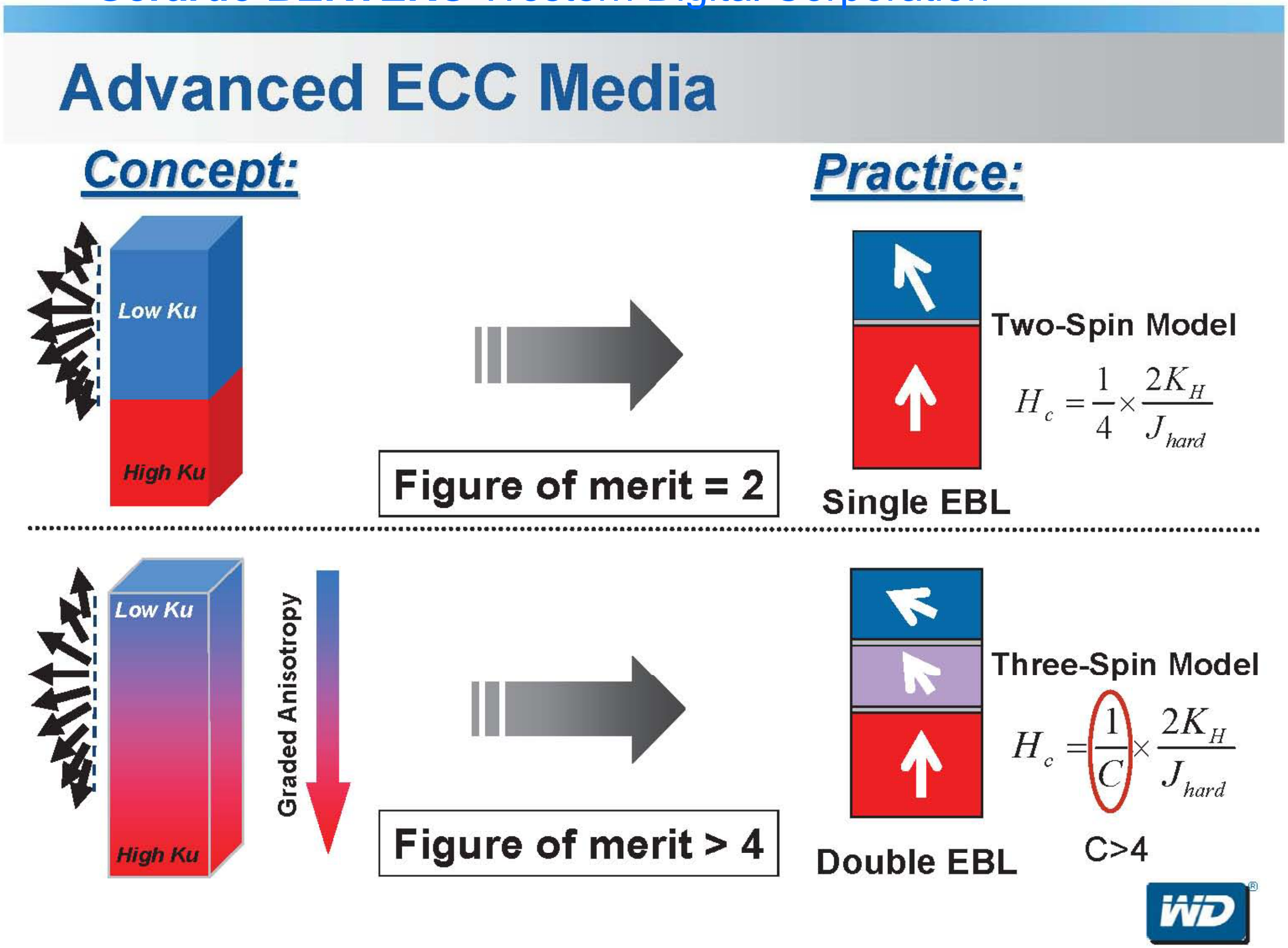

Try exotic. HAMR – Heat Assisted Magnetic Recording

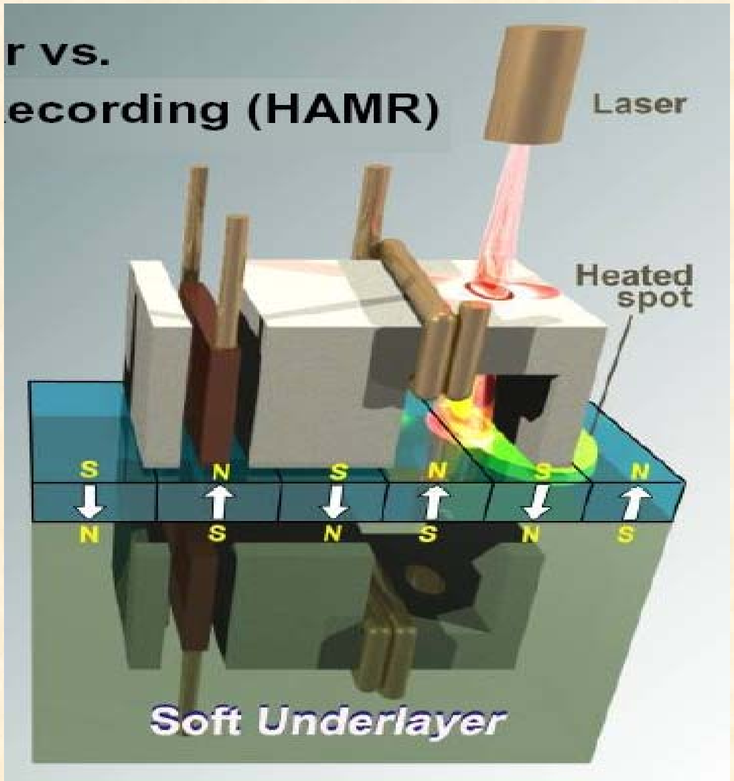

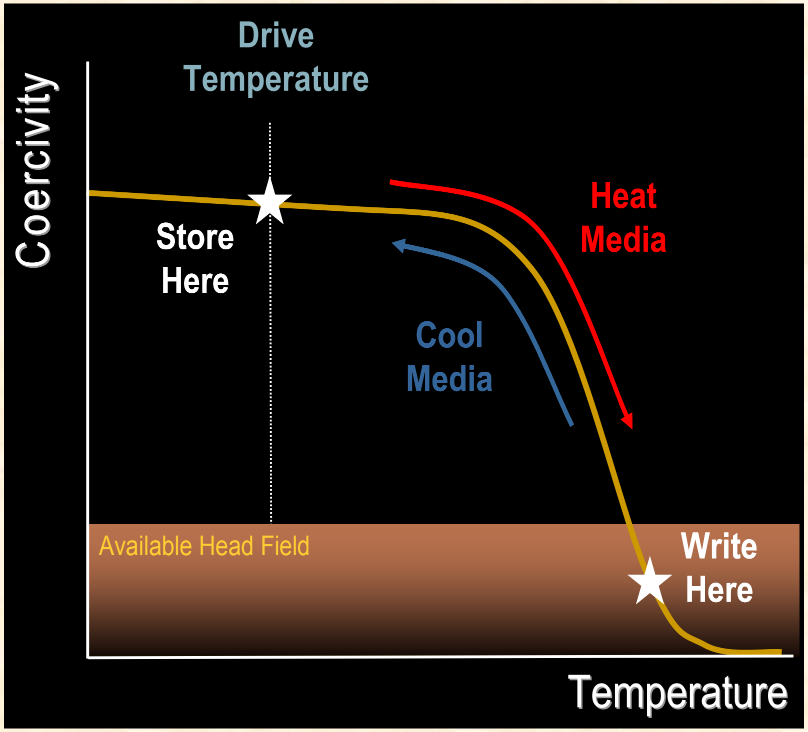

• The challenge in making HAMR work is in creating sufficiently small spatial thermal gradients that will prevent interference between adjacent bits.

Modeling HAMR at the atomic scale using LLG.

J.I. Mercer, M.L. Plumer, J.P. Whitehead, and J. Van Ek, Appl. Phys. Letts. 98, 192508 (2011).

Each grain = 2000 'spins'

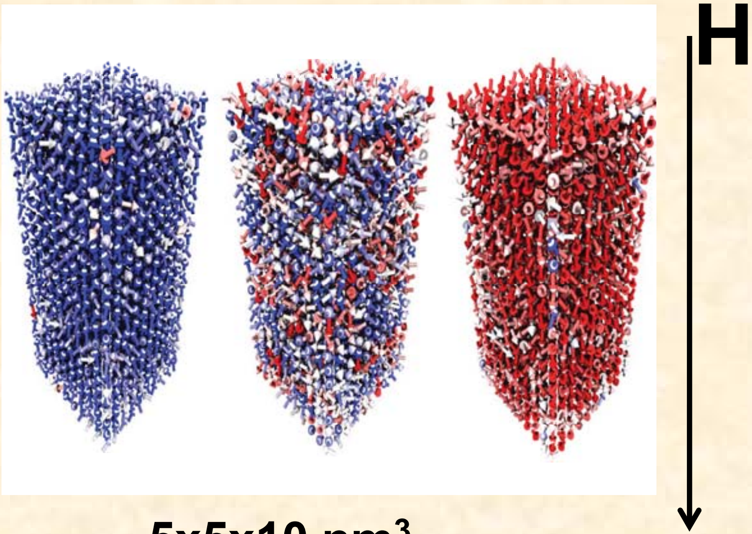

5x5x10 nm^3

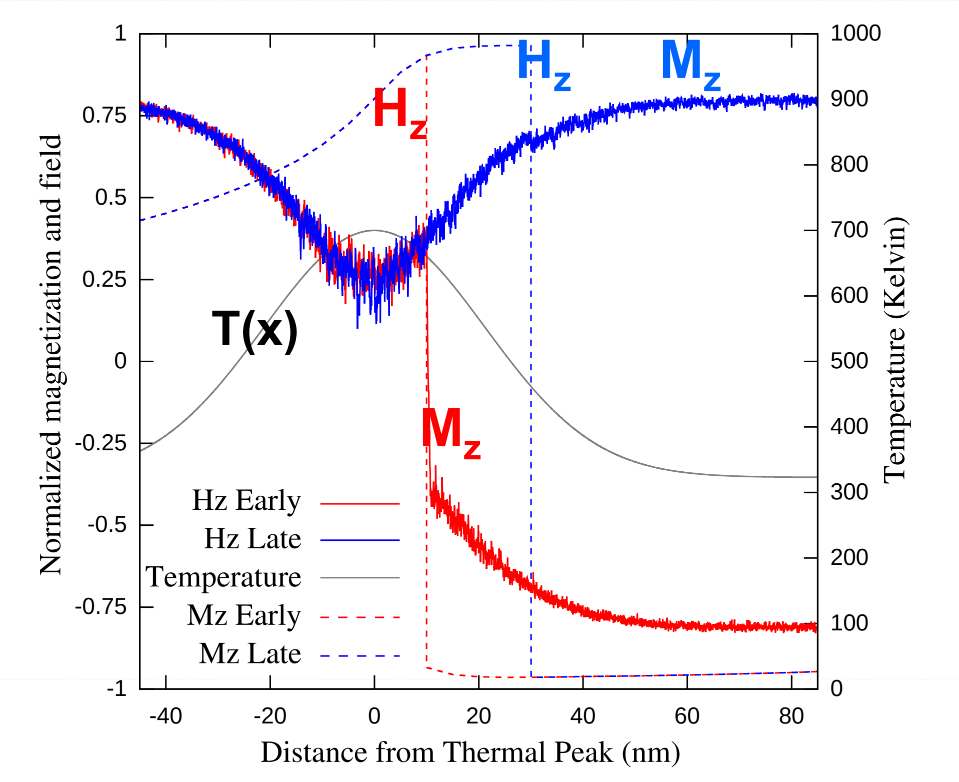

X = Down track direction

Grain reversal is highly non-uniform.

Position of temperature pulse relative to head field maximum is crucial.

<u>Challenges.</u>

- **Control of thermal spot size.**

Try more control:

Bit Patterned Media

Lithographically Patterned Bits:

One bit = one magnetic grain to decrease transition jitter and increase SNR.

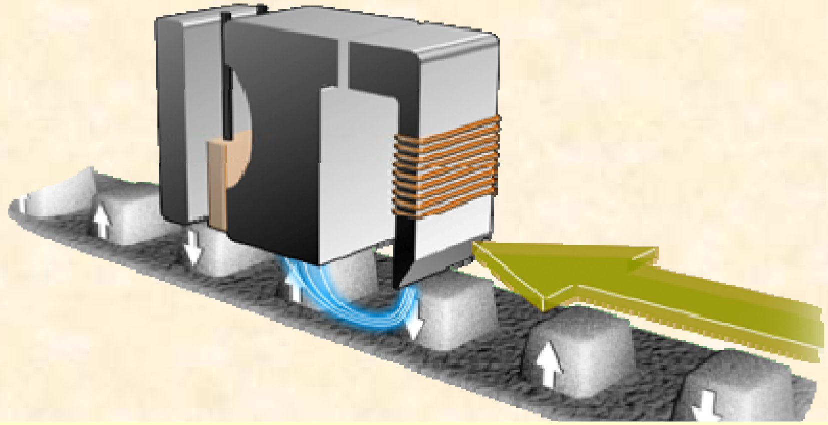

Challenges.

•Making them small enough (1 Tb/in^2 $\Longrightarrow$ 13 nm bits).

•Finding the bits for write and read.

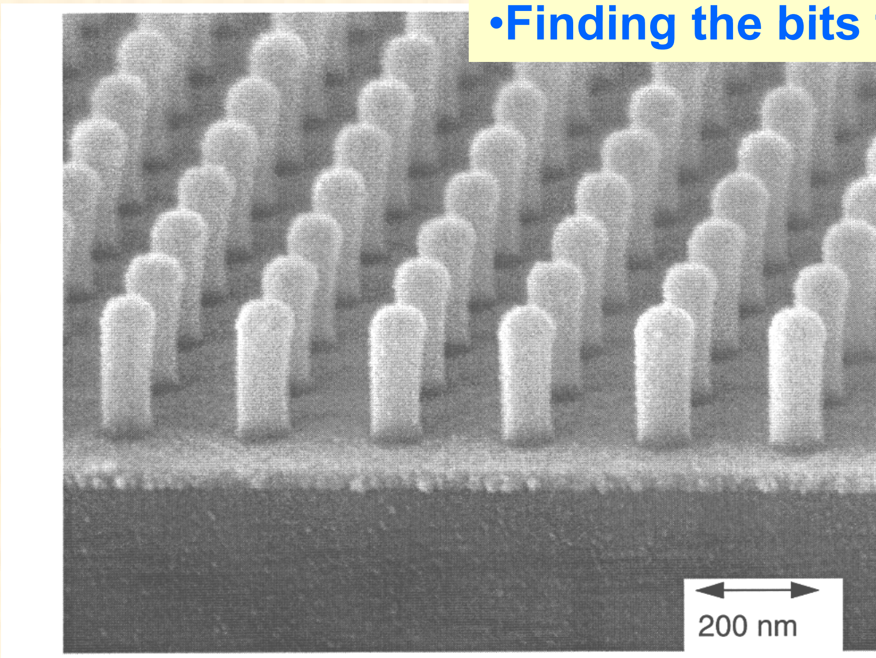

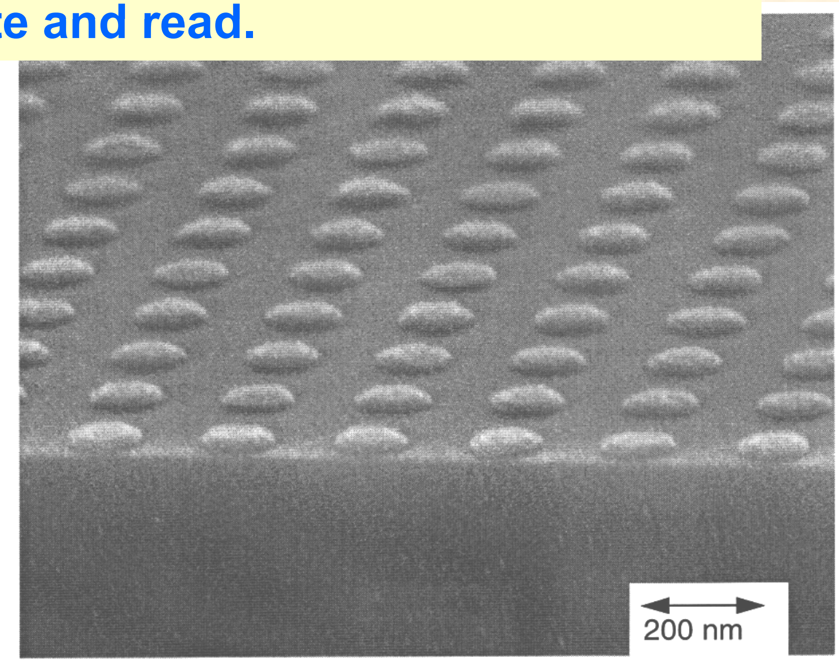

100 nm diameter Co/Cu bilayer dots with 200 nm period

Or more exotic

Self-Assembled Magnetic Nanoparticle Arrays.

An illustration of nanoparticle self-assembly *via* solvent evaporation.

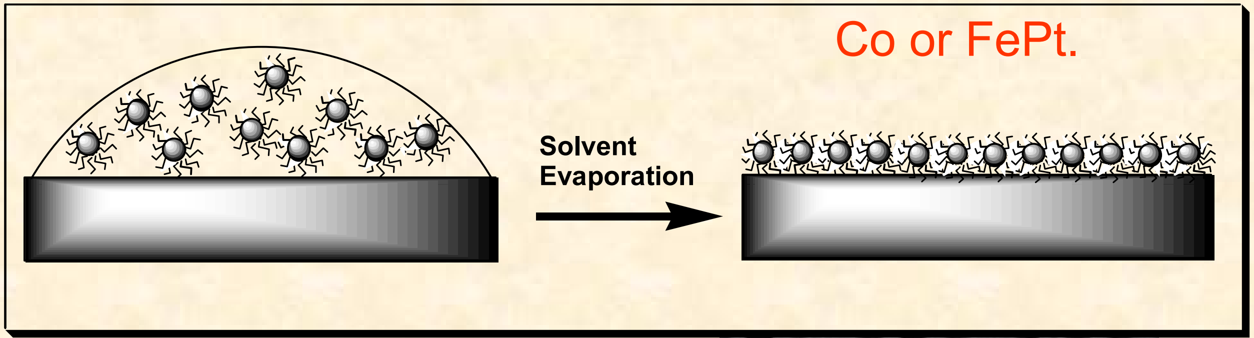

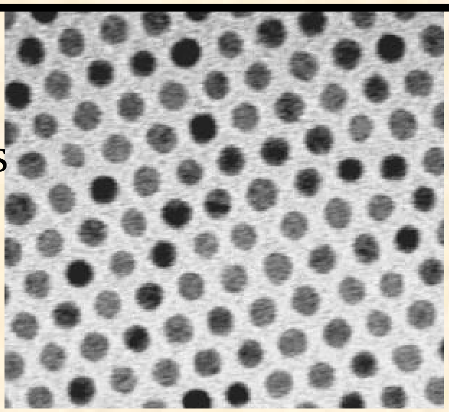

Fig.9.11. TEM images of (a) a 2D assembly, of the 8 nm cobalt nanoparticles on an amorphous carbon surface

Challenges.

- **Control of anisotropy axis distributions.**
- **Uniformity of patterns.**

Conclusions (Part I)

• Large number of new technologies introduced into magnetic recording over the past decade: *GMR, Perpendicular, TMR, ECC*,…

• New paradigms such as *HAMR or BPM* will be very challenging to implement effectively.

• Most likely advances in *Areal Density* in the near future will come from *materials science* and increased understanding of the underlying physics through *numerical simulations.*

Seagate HAMRs hard drives to 1Tb per square inch

Published on 20th March 2012 by Gareth Halfacree

Seagate's HAMR-based hard drives could, it claims, store up to 60TB of data before the technology reaches its upper limit.

Storage giant Seagate has become the first hard drive manufacturer to reach the dizzy heights of one terabit per square inch areal density, using a technology known as heat-assisted magnetic recording (HAMR.)

Designed as a next-generation replacement for perpendicular magnetic recording as used in today's hard drives, HAMR holds the potential for 3.5in hard drives holding as much as 60TB. That, Seagate is quick to point out, would mean more bits in a square inch of hard drive platter than stars in the Milky Way.

PART II.

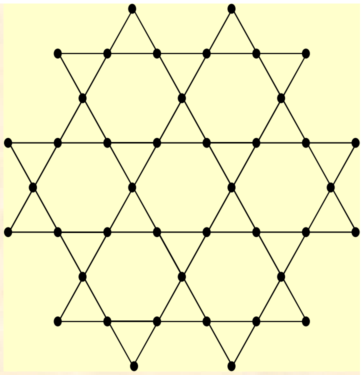

Monte Carlo Simulations of *ABC* stacked Kagomé planes.

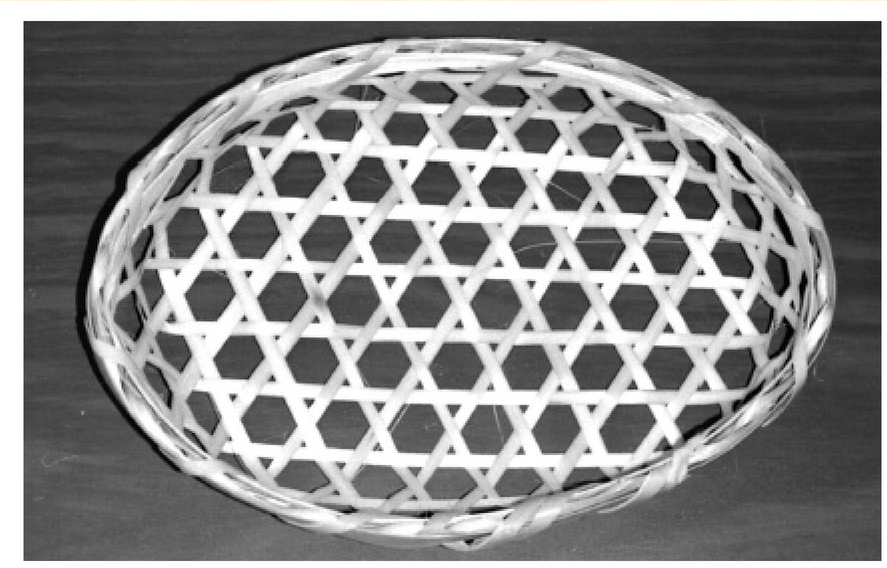

Kagome: The Story of the Basketweave Lattice. M. Mekata, Physics Today Feb. 2003.

First study of magnetic properties: I. Syozi, Prog. Theor. Phys. (1951).

Exchange Pinning in Spin Valves

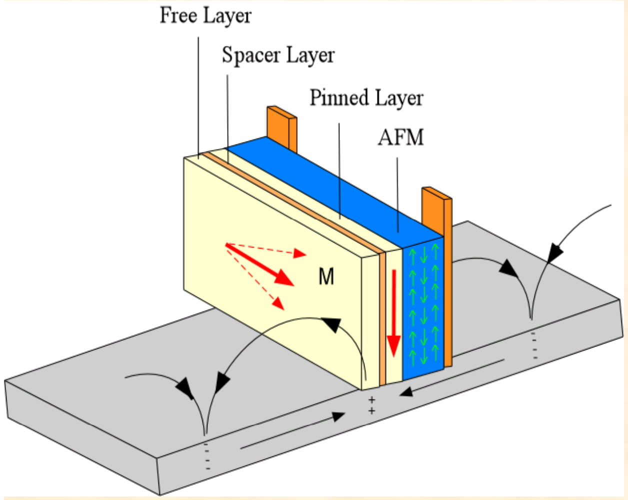

- Pins the Pinned Layer so it does not respond to media bit transition fields.
- Requires T_N >> drive operating temperatures~ 350 K.

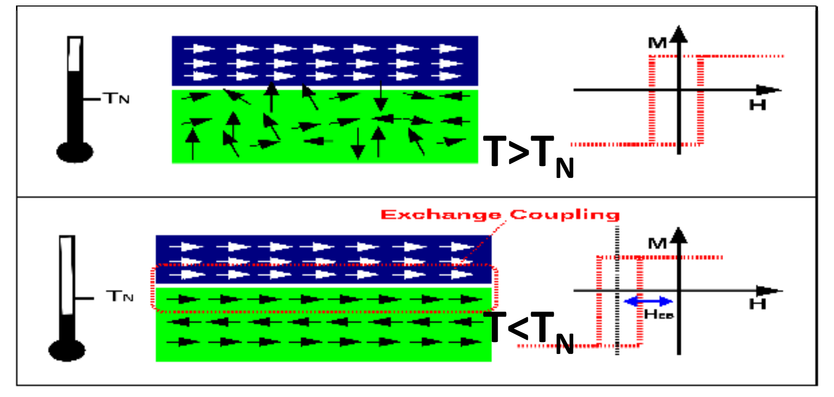

Field cooling to obtain exchange bias.

- Surface spin structure in AF results in a small ferromagentic moment.
- Induces a *uni-directional* field on the PL.
- "After more than 50 years there is still no definitive theory that can account for the observed effects.." K. O'Grady et al., JMMM 322, 883 (2010).

A model...

No obvious mechanism for exchange pinning from compensated surface (M=0).

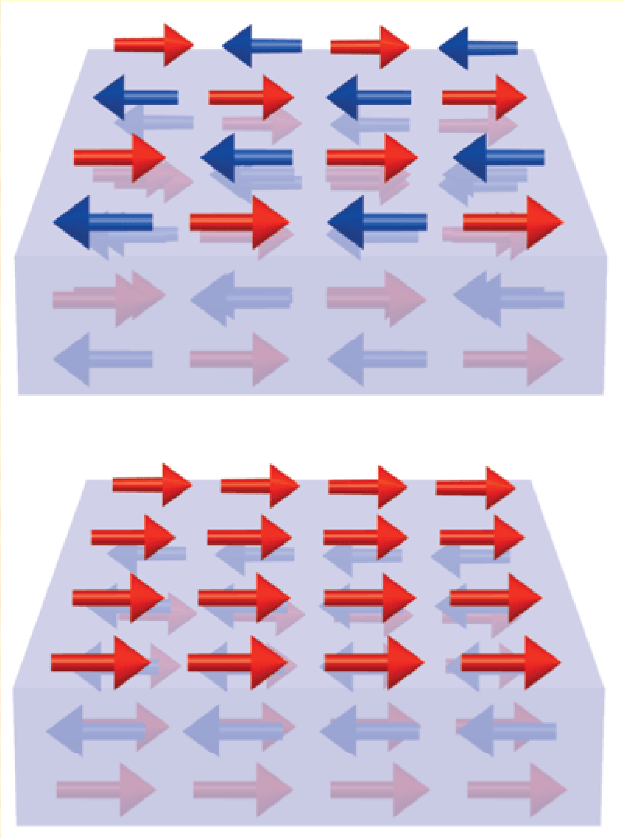

The atomic-scale *Roughness* can create uncompensated spins (red)

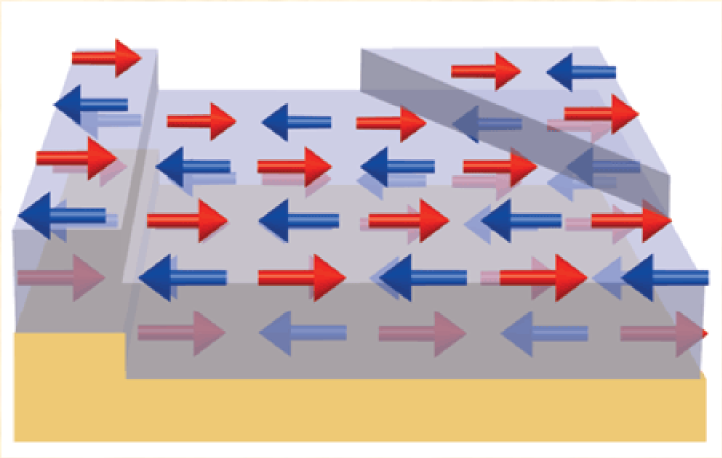

M. Blamire and B. Hickey, Nature Mater. 5, 87 (2006).

J. Spray and U. Nowak, J. Phys. D 39, 4536 (2006).

Another model (Irmy-Ma)...

Domains **involving non-magnetic surface sites.**

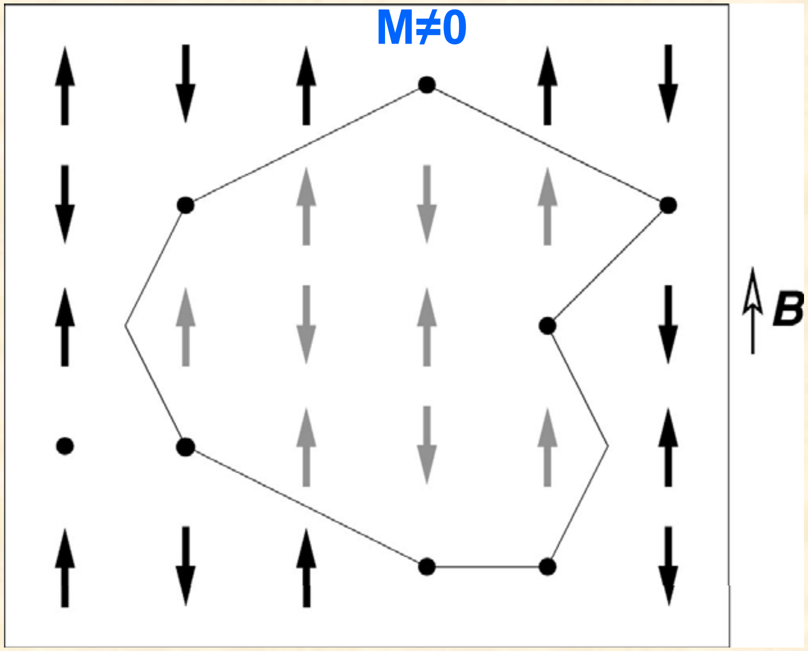

U. Nowak et al PRB 66, 014430 (2002).

M. R. Fitzsimmons et al, PRB 77, 224406 (2008).

Ir-Mn ($IrMn_3$) most popular AF material in spin valves.

$IrMn_3$ = fcc $AuCu_3$ crystal structure. Also: $RhMn_3$ and $PtMn_3$

I. Tomeno et al J. Appl. Phys. 86, 3853 (1999).

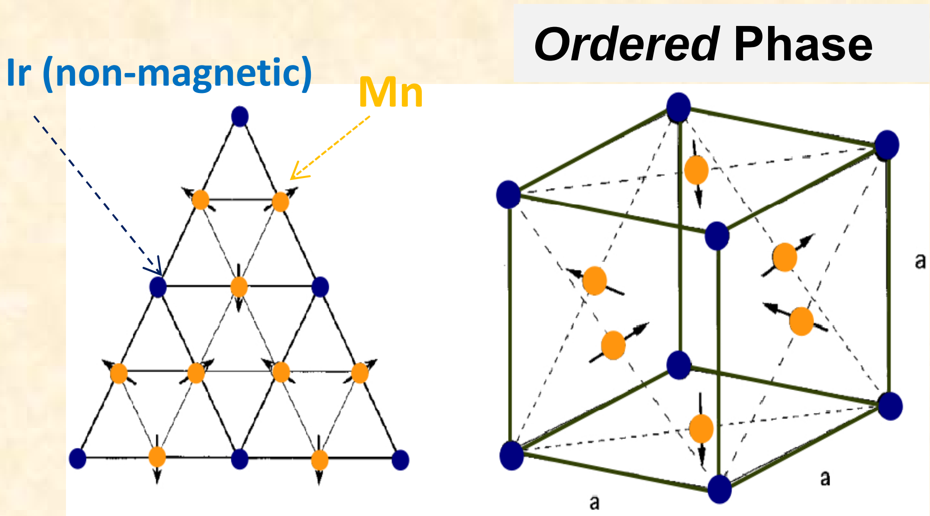

Neutron diffraction on bulk single crystals.

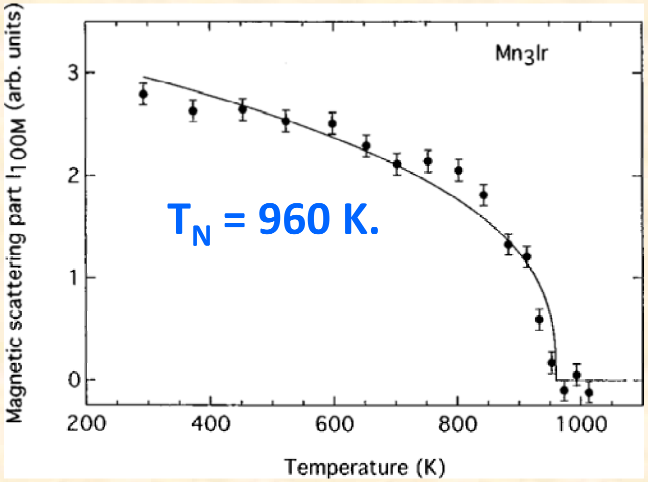

'T1' ⇒ 2D spin structure

Very large T_N.

fcc lattice = *ABC* stacked triangular layers ⊥ <111>

Ordered $IrMn_3$ ⟹

fcc Kagomé lattice = *ABC* stacked Kagomé layers ⊥ <111>

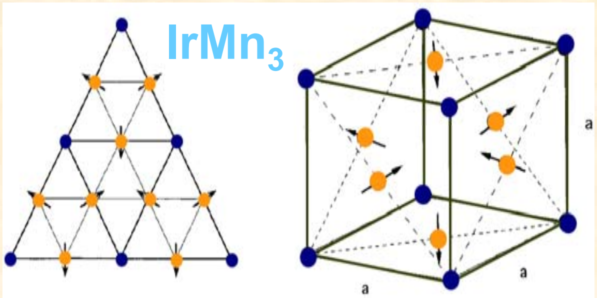

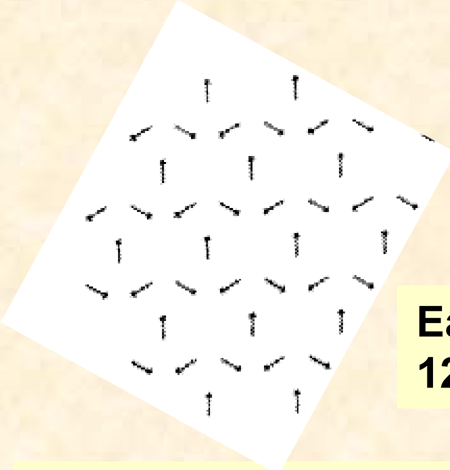

2D Kagomé: Highly Frustrated AF

Each triangle forms 120^0 spin structure

Applied Physics: 'T1' spin structure (no mention of Kagomé).

E. Krén et al, Phys. Lets. 20, 331 (1966).
I. Tomeno et al J. Appl. Phys. 86, 3853 (1999).

Thin films of $IrMn_3$ form <111> planes.

Basic Physics: 'q=0' spin structure (no mention of 'T1').

A.B. Harris et al, PRB 45, 2899 (1992).

- **2D Heisenberg model exhibits coplanar spin structure.**
- **Macroscopic spin degeneracy at T=0**

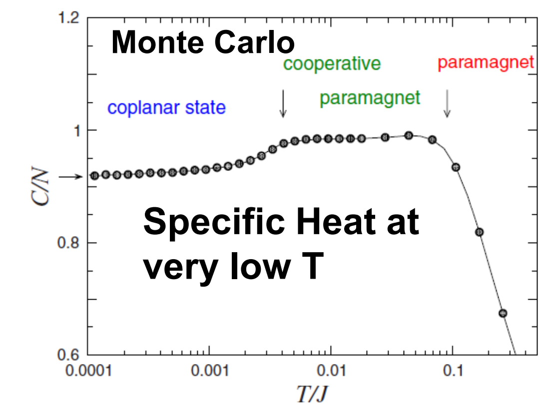

FIG. 3. (Color online) Temperature dependence of the specific heat for a kagome lattice cluster with $L=36$. The horizontal arrow denotes the value $C/N=\frac{11}{12}$. The two vertical arrows indicate boundaries between three different regimes.

M. Zhitomirsky, PRB 78, 094423 (2008).

Monte Carlo simulations of the (3D) fcc Kagomé lattice.

Heisenberg and XY Models with NN Exchange J Only.

V. Hemmati, M.L. Plumer, J.P. Whitehead, and B.W. Southern, PRB 86, 104419 (2012).

***ABC* stacked** **View along <111>**

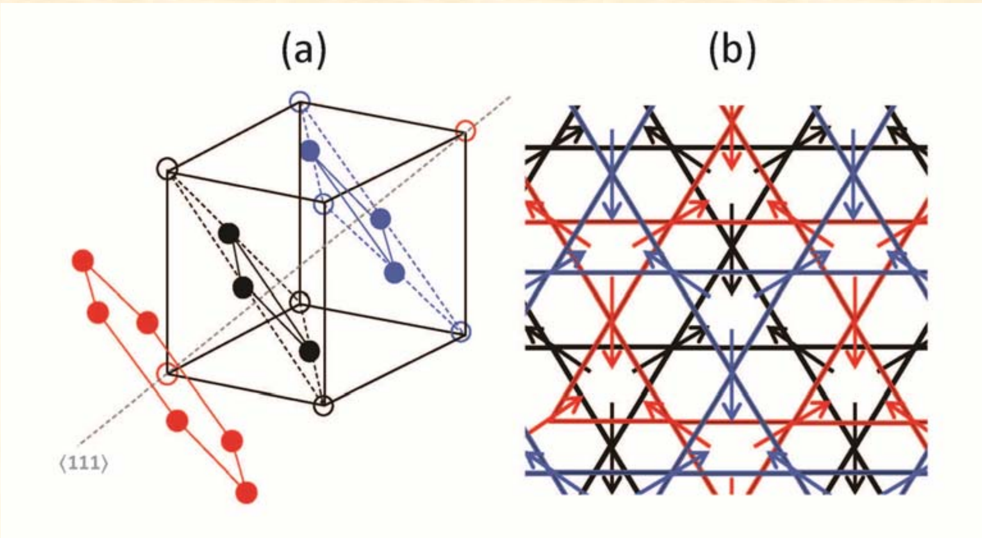

J ⇒ **4 NN in-plane**
+ 2 NN above + 2 NN below

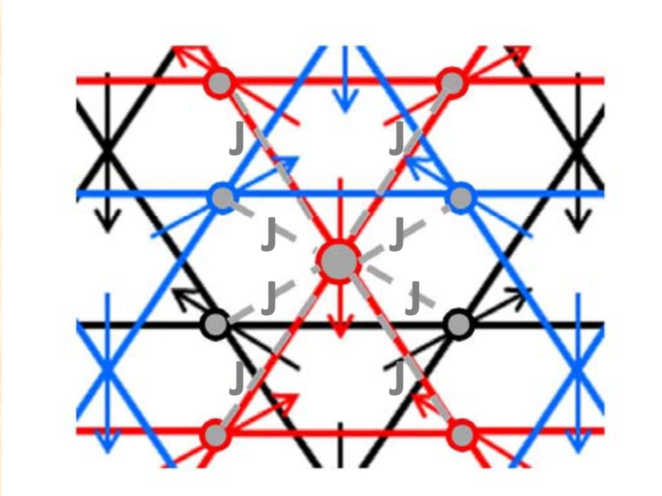

- Recall fcc = ABC stacked triangular layers with 12 NN^s.
- Regular fcc AF with NN Heisenberg exchange shows first order transition to a collinear state.

Ground State from simulations:
- Each layer has ‘q=0 spin’ structure.
- 120^0 between all 8 NNs.

Monte Carlo simulations of the fcc Kagomé lattice.

Energy and Specific Heat.

- *Standard Metropolis MC.*
- *L* layers of ABC stacked *LxL* Kagomé planes with PBC.
- *L* = 12, 18, 24, 30, 36, 60 with MCS = $10^6 - 10^7$
- *Cooling, Heating and Independent* temperature runs.

Energy **L=24** **Specific Heat**

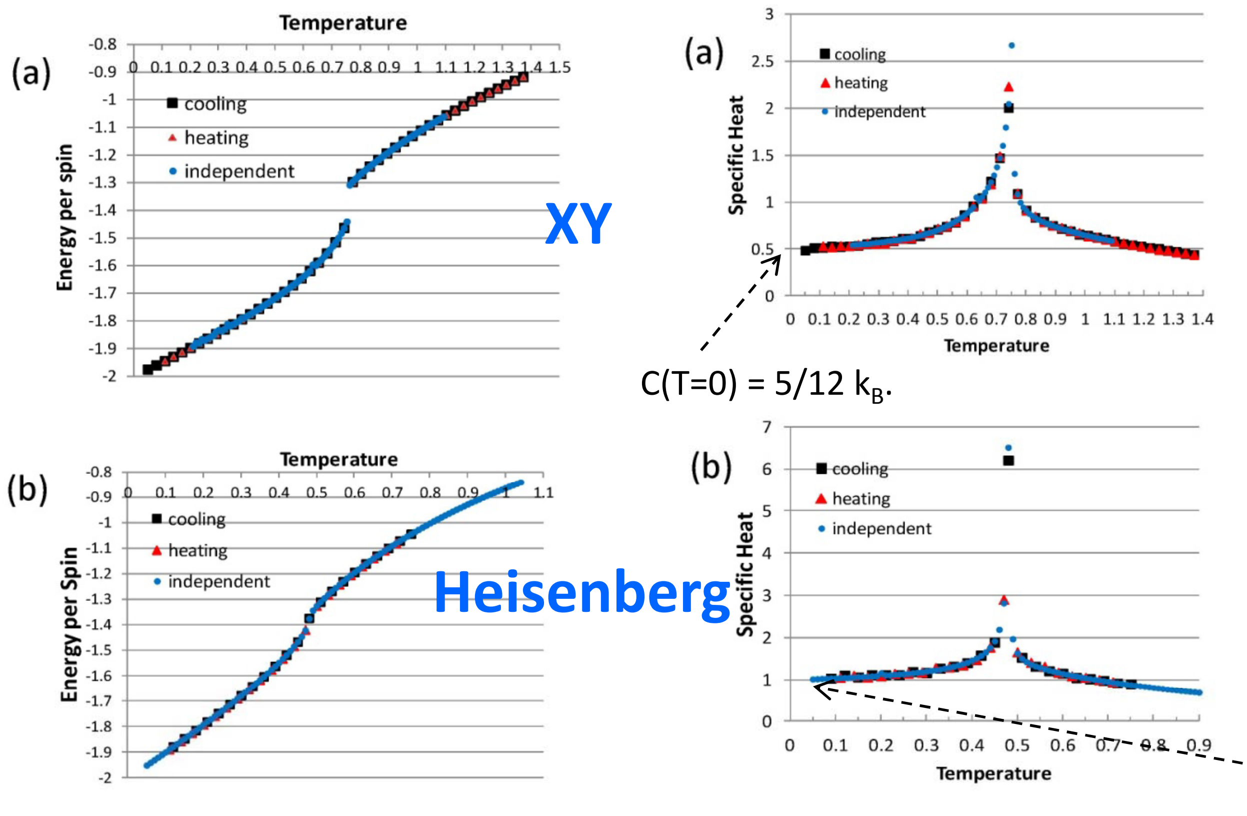

- **All three types of simulations yield equivalent results.**
- **For XY model, T_N = 0.760 and appears to be strongly first order.**
- **For Heisenberg model, T_N = 0.476 and could be first order.**

Monte Carlo simulations of the fcc Kagomé lattice.

Order of the Transitions.

Heisenberg Energy.

L=36.

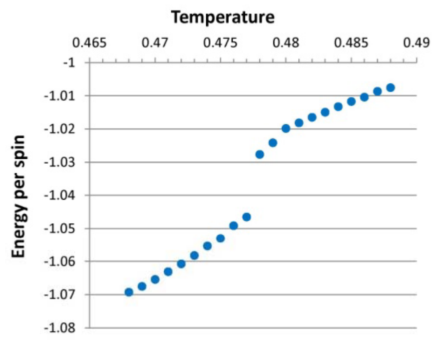

Discontinuity in Heisenberg energy clearer at L=36.

Energy Histograms near T_N

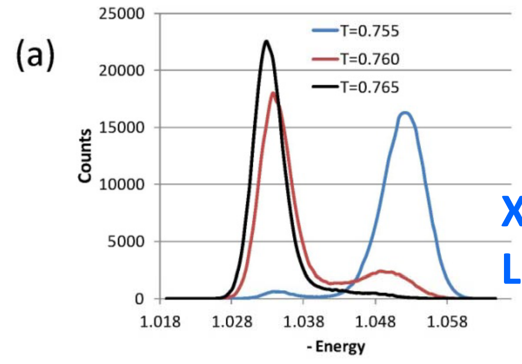

XY.
L=24.

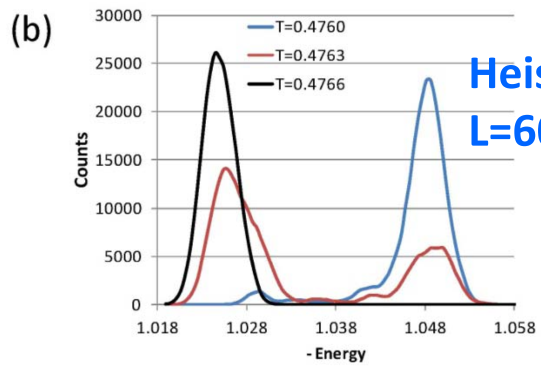

Heisenberg.
L=60.

Indicate energy gap between disordered and ordered phases for *both* models.

Binder *Heisenberg* Energy Cumulant near T_N.

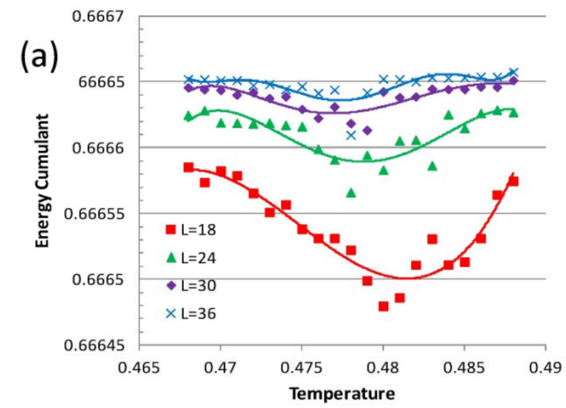

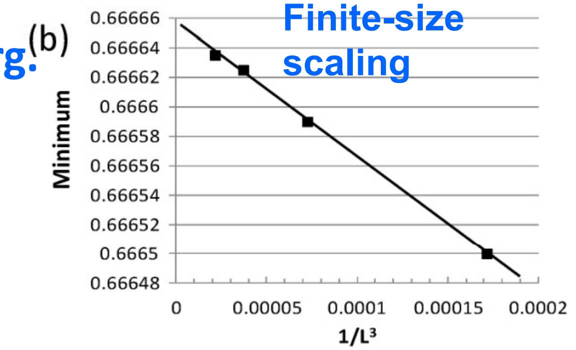

Finite-size scaling

Inconclusive: Could be 2/3, or just close.

Monte Carlo simulations of the fcc Kagomé lattice.

q=0 Order Parameter and Susceptibility.

Order Parameter **L=24** **Susceptibility**

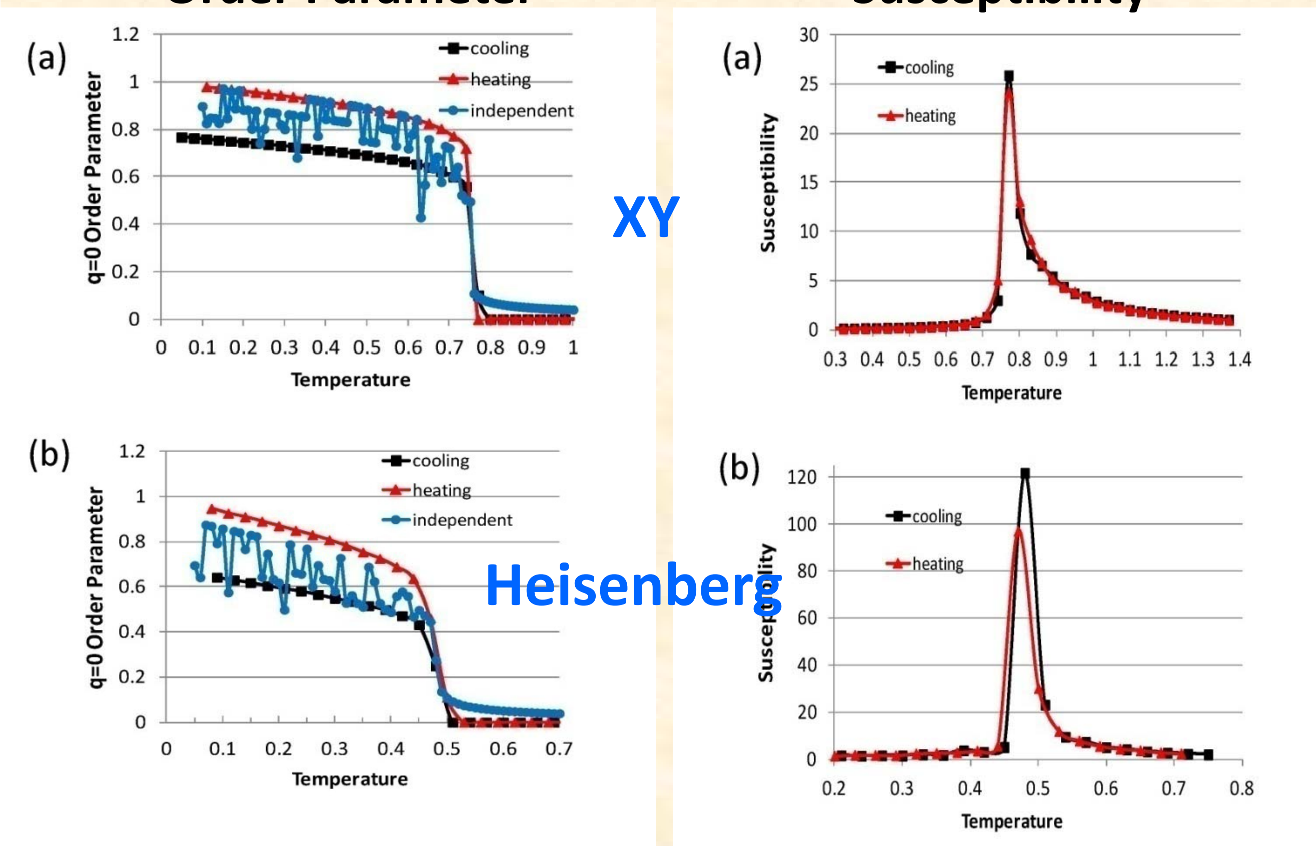

- **Heating runs start at T=0 from fully order q=0 state.**

- **Order Parameter and Susceptibility show strong dependence on simulation mode (heating, cooling or independent temperature) and fluctuates between values, *in contrast with energy and specific heat.***

- **This feature is due to Kagomé-lattice spin degeneracies**

Monte Carlo simulations of the fcc Kagomé lattice.

Spin Degeneracies.

Define 3 ferromagnetic sub-lattice magnetization vectors: black, blue red.

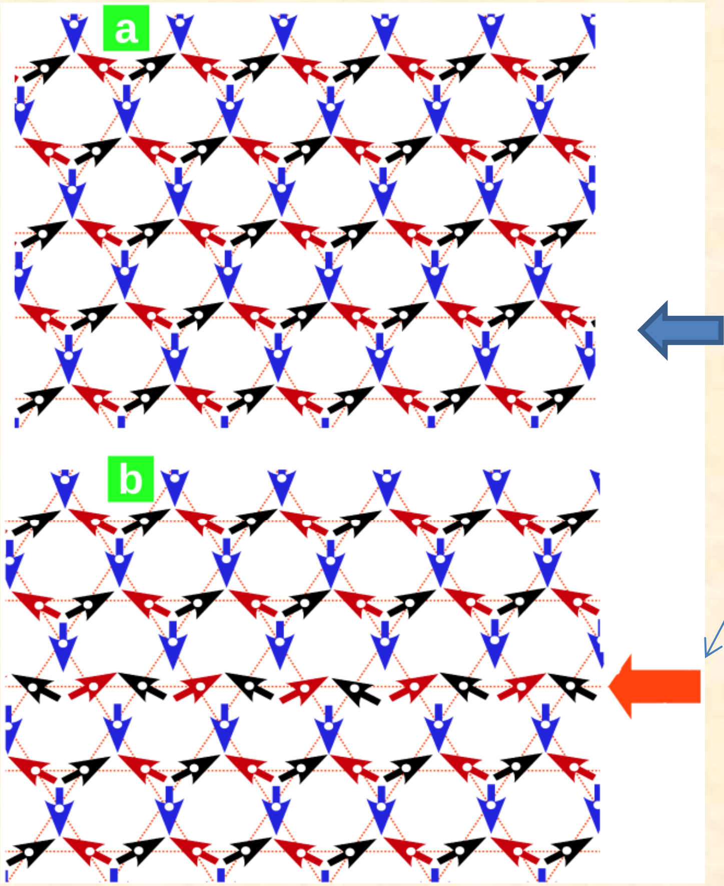

'q=0' magnetic structure ⇒ 3 spins around each triangle at 120^0

In 2D, can switch direction of two of the sub-lattices vectors in a row (e.g., **black** ⟷ **red**) with no change in energy.

In 3D, can switch direction of two of the sub-lattices vectors in a plane with no change in energy

Monte Carlo simulations of the fcc Kagomé lattice.

Spin Degeneracies.

Enumerate all possible switches for L=24 and determine size of ground-state sub-lattice moment:

$$M_\eta = \frac{\sqrt{\left(\frac{1}{4}\,L^3 - \frac{3}{2}\,n\right)^2 + \left(\frac{\sqrt{3}}{2}\,n\right)^2}}{\frac{3}{4}\,L^3}$$

$L^3/8 \le n \le L/2$

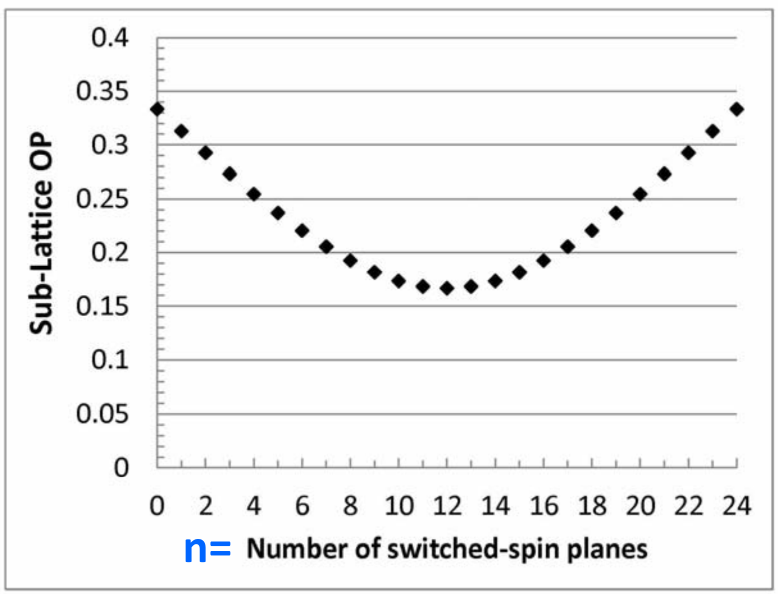

Three different MC *cooling* runs (different random initial configuration).

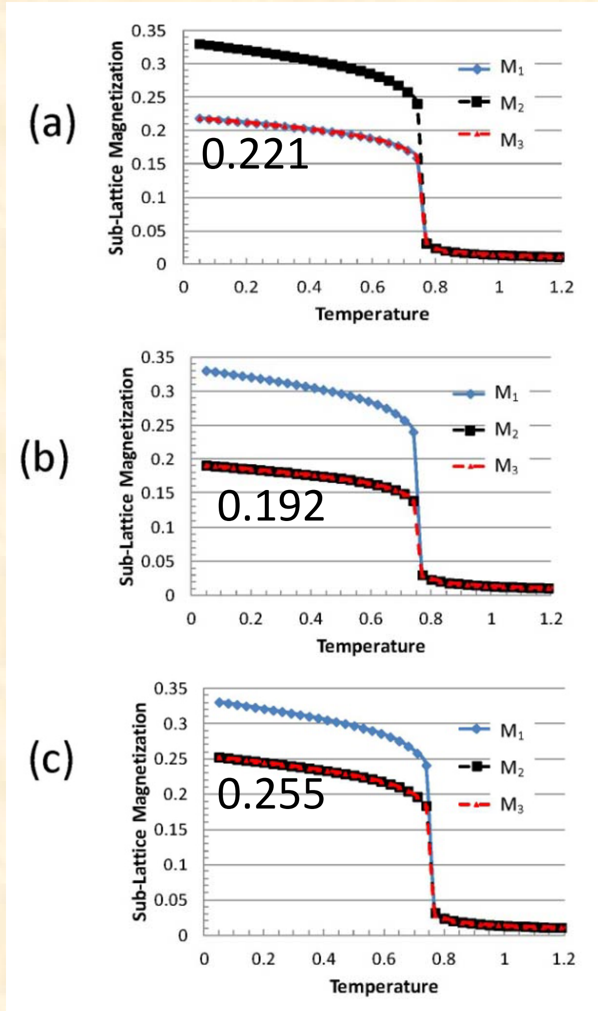

- **One sub-lattice is always fully saturated.**
- **The other two randomly approach (T=0) predicted values.**

Monte Carlo simulations of the fcc Kagomé lattice.

Add anisotropy

L. Szunyogh et al PRB 79, 020403 (2009)

$$H = -\frac{1}{2}\sum_{i\neq j} J_{ij}\vec{S}_i\vec{S}_j - \frac{K_{\text{eff}}}{2}\sum_i (\vec{S}_i \cdot \vec{n}_i)^2,$$

Effective local anisotropy axes (similar to spin-ice pyrochlore tetrahedrons).

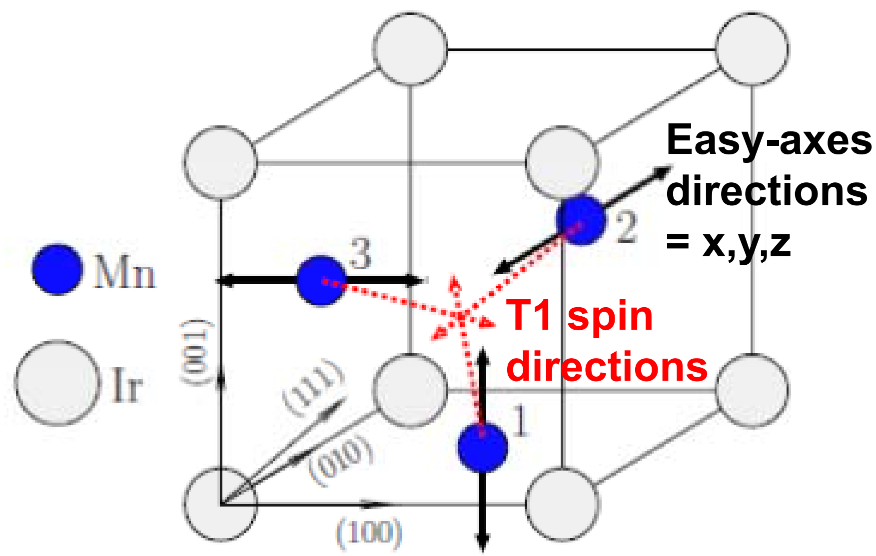

Initial MC results show that anisotropy:

- removes degeneracy

- induces an out-of-plane ferromagnetic moment

-drives the transition to be continuous .

Mn moments are *not* aligned in the easy-axes directions for the coplanar T1 spin structure.

Relation to Exchange Pinning.

XRD, and DFT calculations of $IrMn_3/CO_4$ and $IrMn_3/Fe_4$ interface spin structures. *H. Takahashi et al, J. Appl. Phys. 110, 123920 (2011)*

Interaction with ferromagnetic layer induces a net moment in surface Mn spins.

Interface

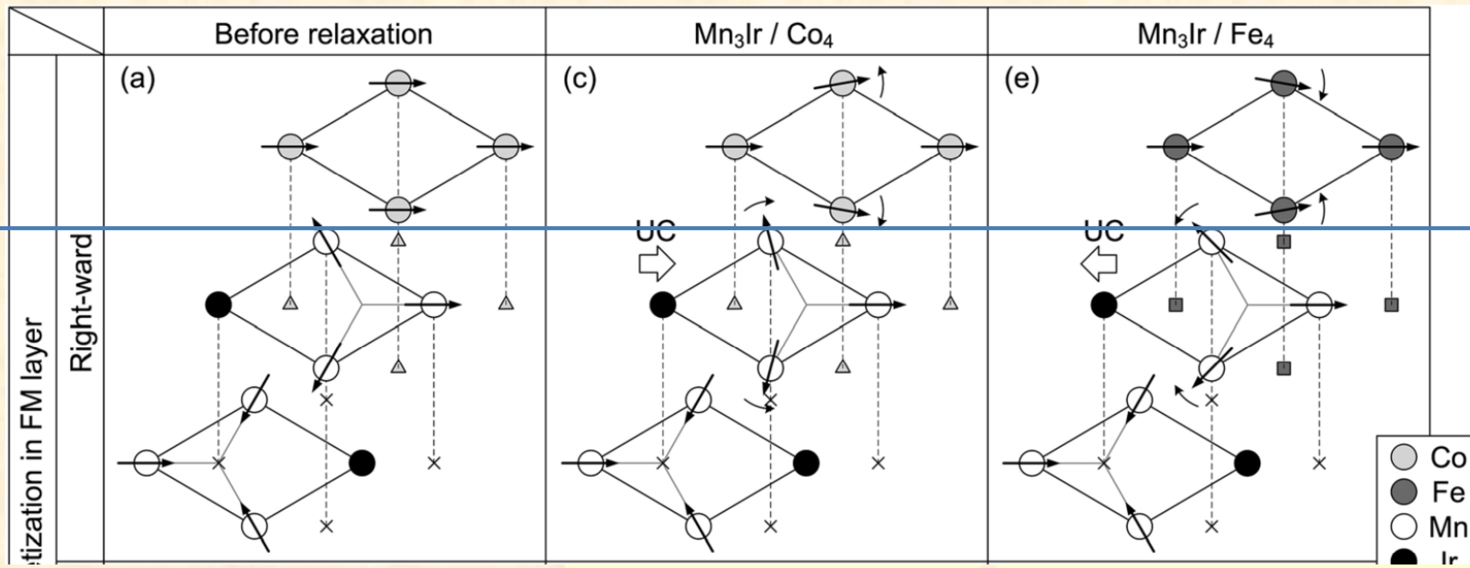

Mn moments rotate toward Co-moments

Mn moments rotate away from Fe-moments

Relation to exchange pinning?

Phase transitions in the fcc Kagomé lattice

Summary and Conclusions

• 3D fcc Kagomé lattice with NN exchange only shows LRO transitions of the ‘q=0’ type at T_N=0.760 J for the XY model and T_N = 0.476 J for the Heisenberg model.

• XY model ⇒ Strongly first order.
• Heisenberg model ⇒ Probably weakly first order.
• Mean field theory ⇒ Continuous transition in both cases.

• Spin degeneracies of the 2D model persist in the 3D case ⇒ Order-by-disorder?

Future work:
- effects of anisotropy.
- thin films and surface effects
- add a ferromagnetic layer and dipole interactions.
- ⇒ ***Exchange Pinning?***

Evidence for first-order transition in $IrMn_3$: χ vs T

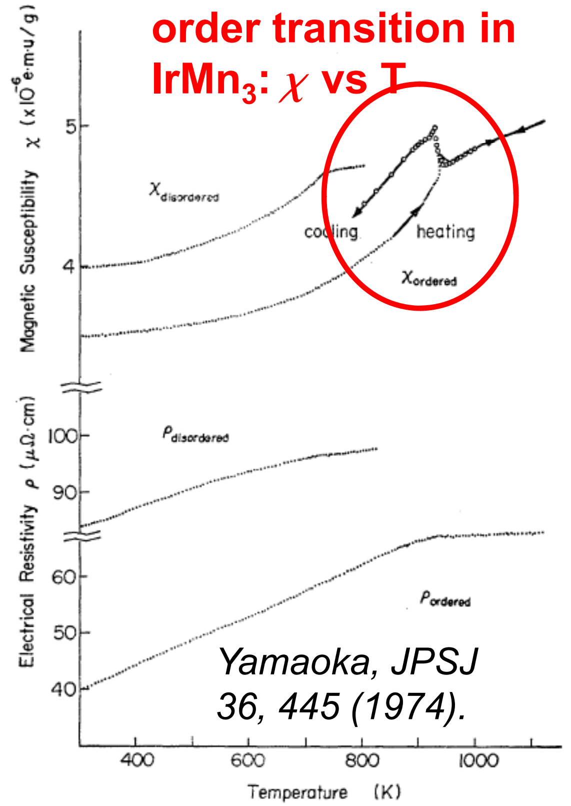

Fig. 5. Temperature dependences of magnetic susceptibility χ and electrical resistivity ρ of the partially ordered (S=0.83) alloy compared with those of the disordered (S<0.08) alloy with x=0.256. Open circles indicate the cooling process.

Magnetic recording, and phase transitions in the fcc Kagomé lattice:

Collaborations and Support: Who's doing the work and who's paying for it.

- **Vahid Hemmati (MSc graduate)** Memorial University
- **Jason Mercer (PhD student)** Memorial University
- **Martin Leblanc (PhD student)** Memorial University
- **John Whitehead (professor)** Memorial University
- **Byron Southern (professor)** University of Manitoba
- **Johannes Van Ek (scientist)** Western Digital Corporation

- **Natural Sciences and Engineering Council of Canada**
- **Western Digital Corporation**
- **Canada Foundation for Innovation**
- **Atlantic Centre of Excellence Network**

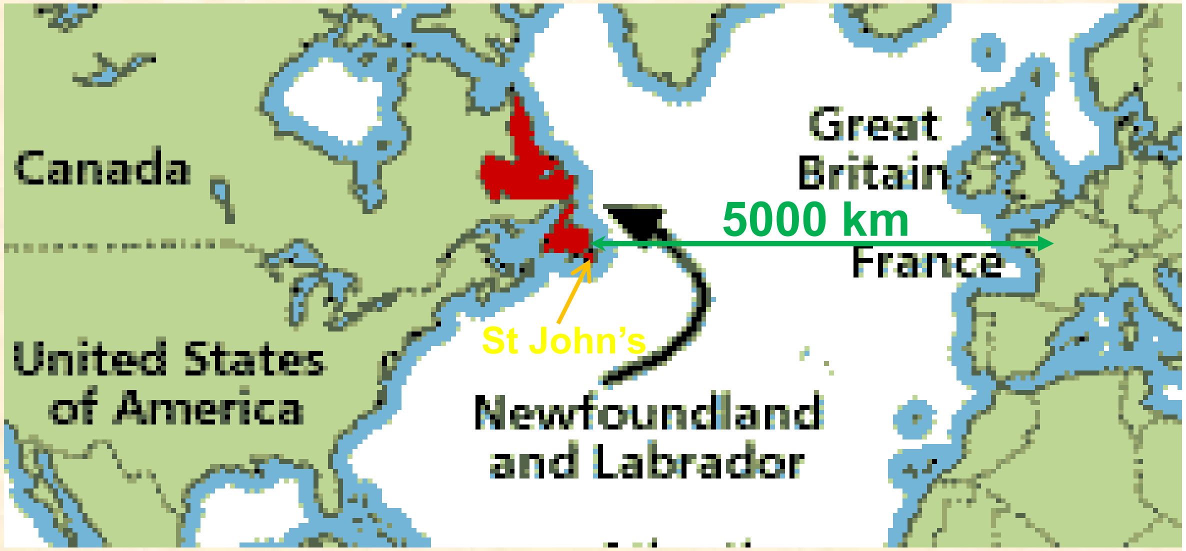


Island of Newfoundland
St. John's
Fortune Bay
Saint Pierre and Miquelon
iquelon-Langlade
Saint-Pierre

Anisotropy vs Exchange

$$H = -\frac{1}{2}\sum_{i \neq j} J_{ij}\vec{S}_i\vec{S}_j - \frac{K_{\text{eff}}}{2}\sum_{i}(\vec{S}_i \cdot \vec{n}_i)^2,$$

Black = easy axes

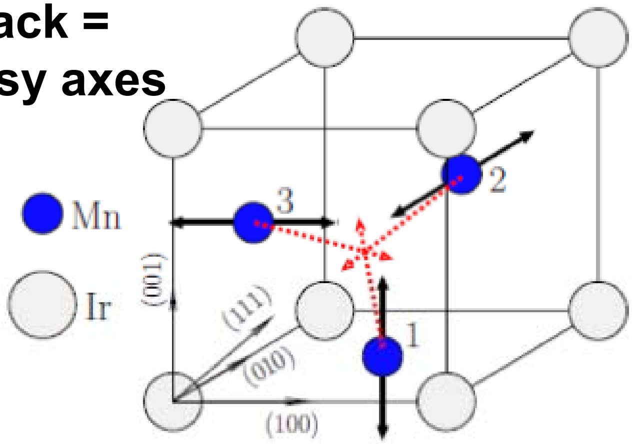

T_c vs K

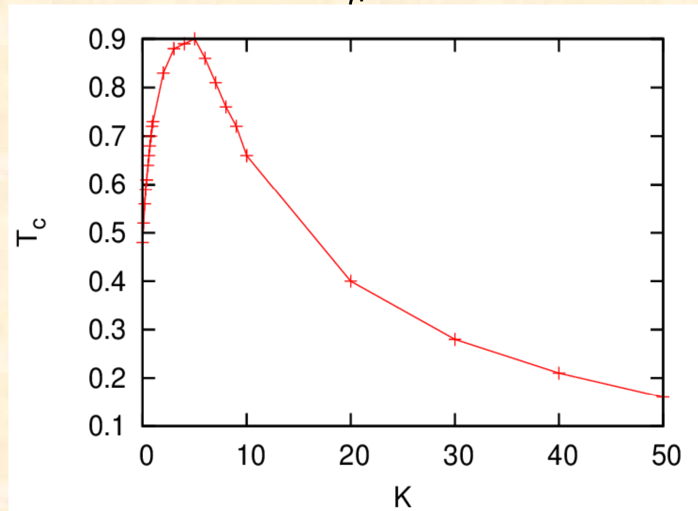

Angle between spins:
No longer 120^0 coplanar

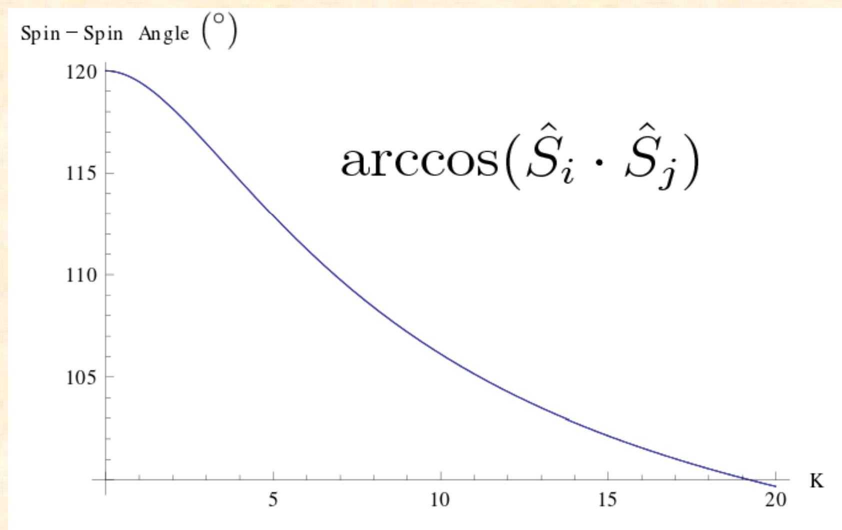

Micromagnetics: Reader Efficiency vs Sensor Height.

100% efficiency = full 180^0 rotation

22% efficiency

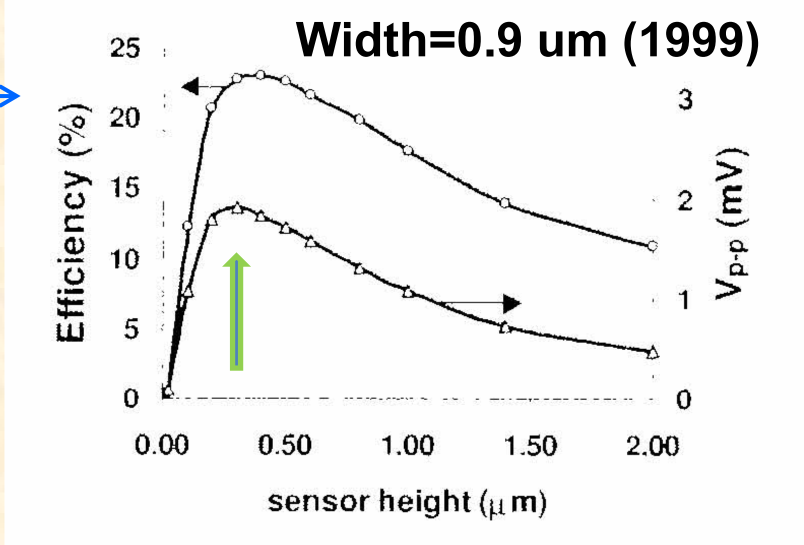

Present reader widths ~ 50 nm

Maximum efficiency for Height/Width ~ 1/3

Still True Today.

Anisotropy Effect

- Anisotropy removes continuous degeneracy
- Adds its own 8-fold degeneracy
- Spins are no longer in-plane -
  ferromagnetic component

Cooling runs

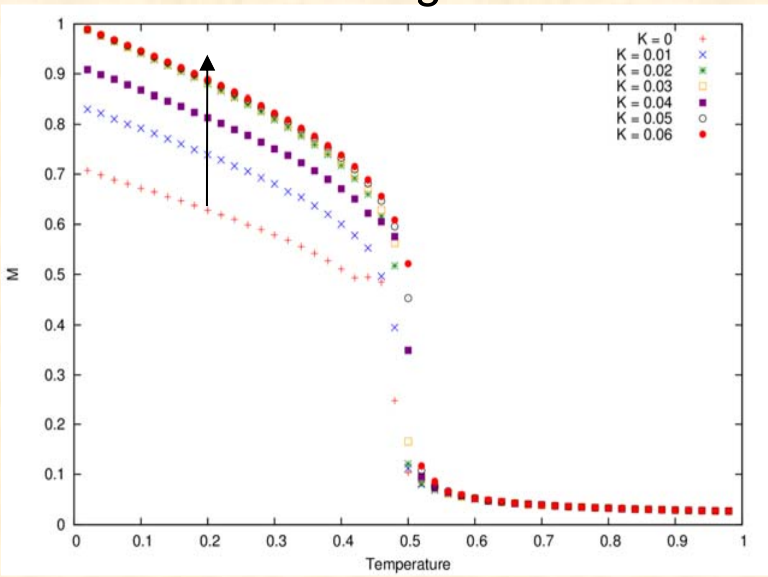

Out-of-plane Magnetization vs K

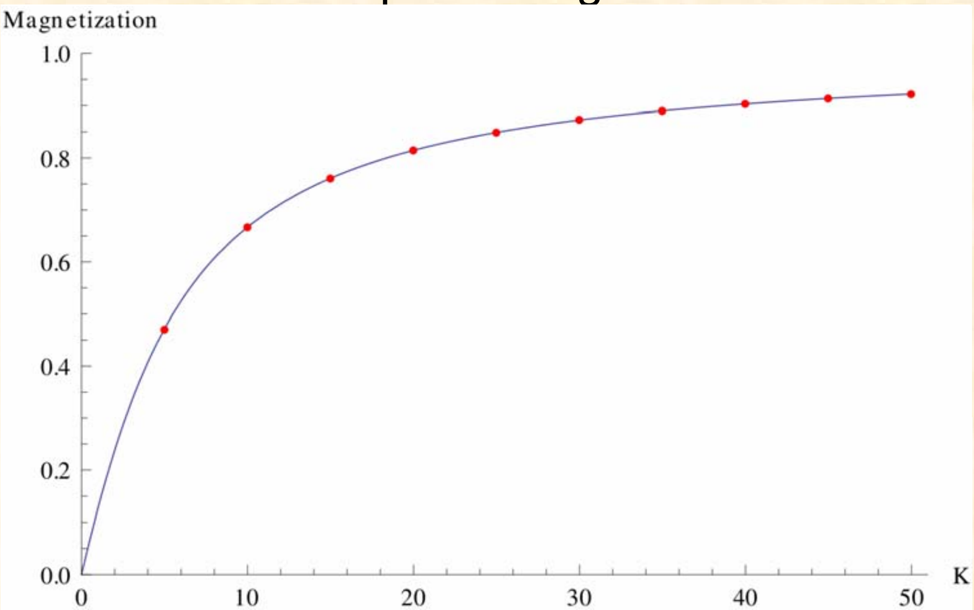

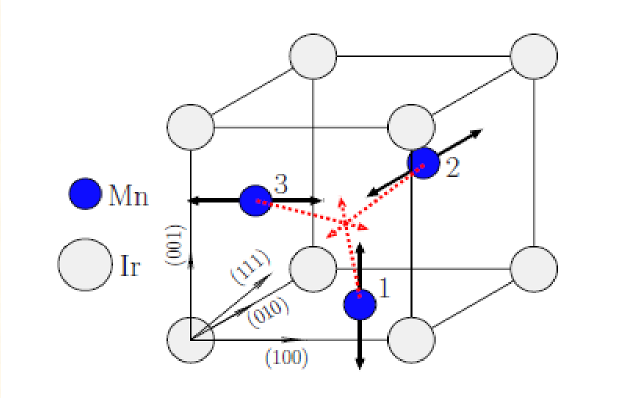

Anisotropy Effect

- Anisotropy removes continuous degeneracy
- Adds its own 8-fold degeneracy
- Spins are no longer in-plane - ferromagnetic component

Cooling runs

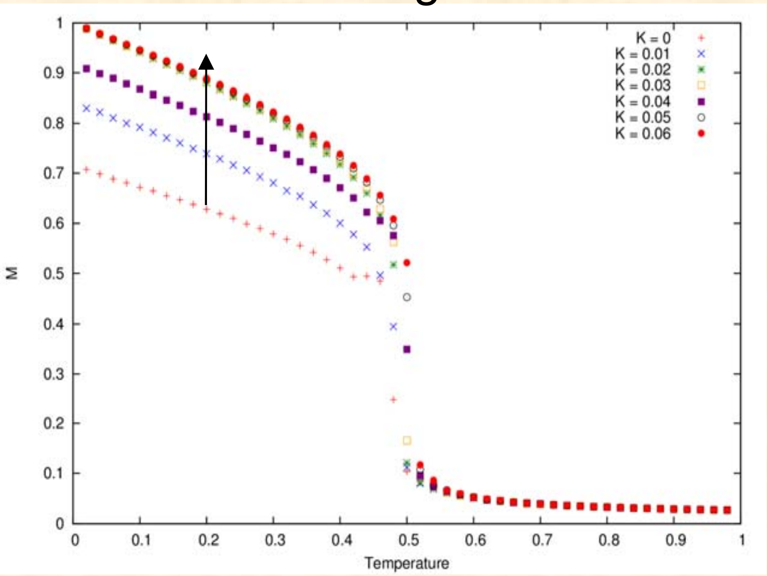

Out-of-plane Magnetization vs K

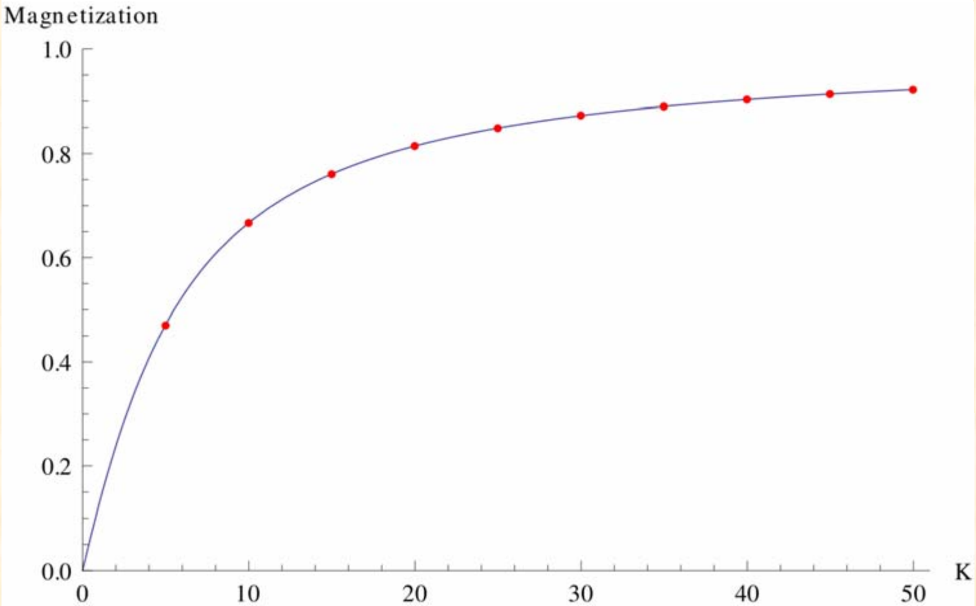

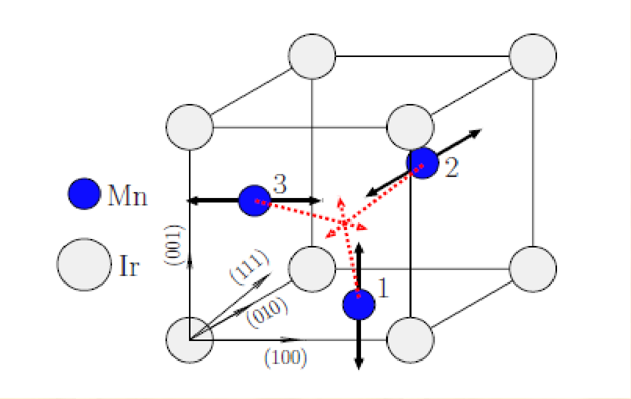

Anisotropy Effect

- Anisotropy removes continuous degeneracy
- Adds its own 8-fold degeneracy
- Spins are no longer in-plane - ferromagnetic component

Cooling runs

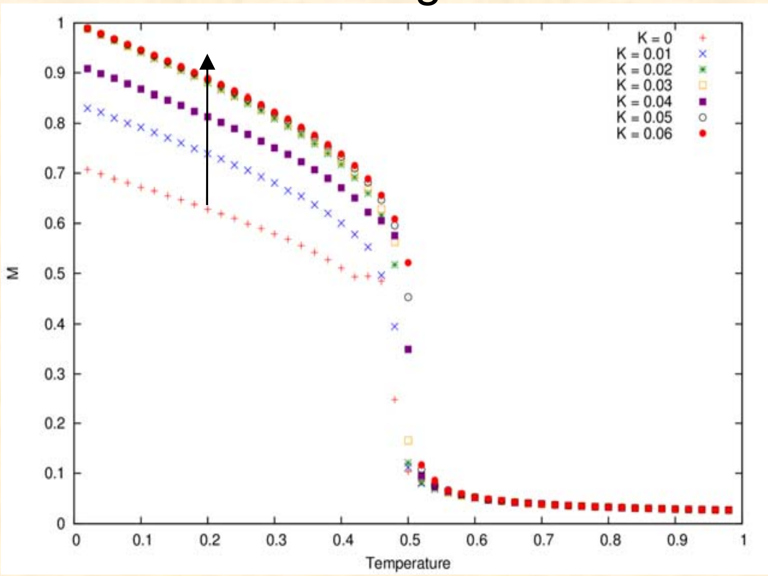

Out-of-plane Magnetization vs K

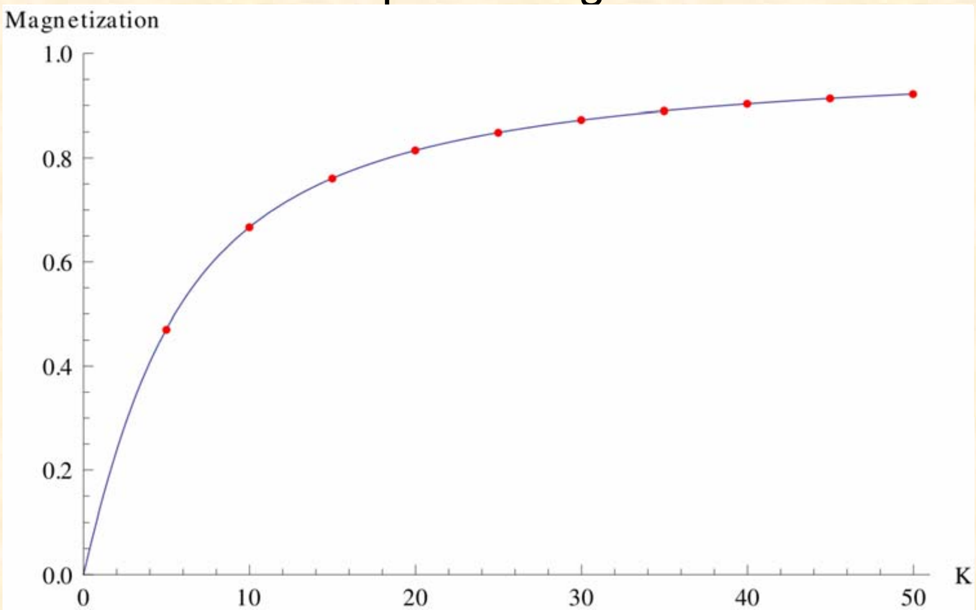

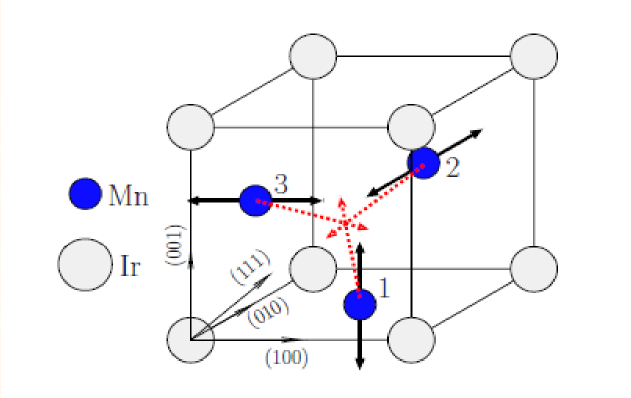

3D Kagome Energy, $K_{eff} > 0$

Specific Heat to find T_N

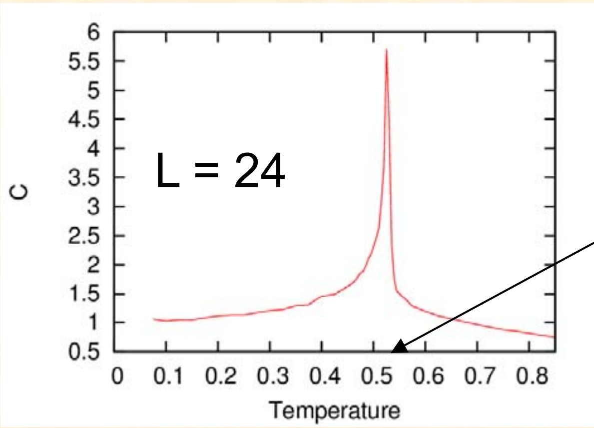

$K_{eff} = 0.1$

$T_N = 0.5250$
(0.4765 for $K_{eff} = 0$)

Energy Histogram near T_N

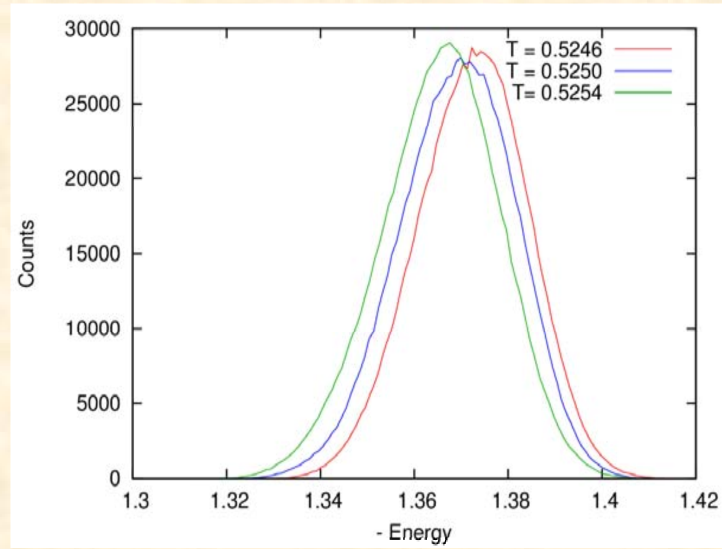

$K_{eff} = 5$

$T_N = 0.9050$

L = 36

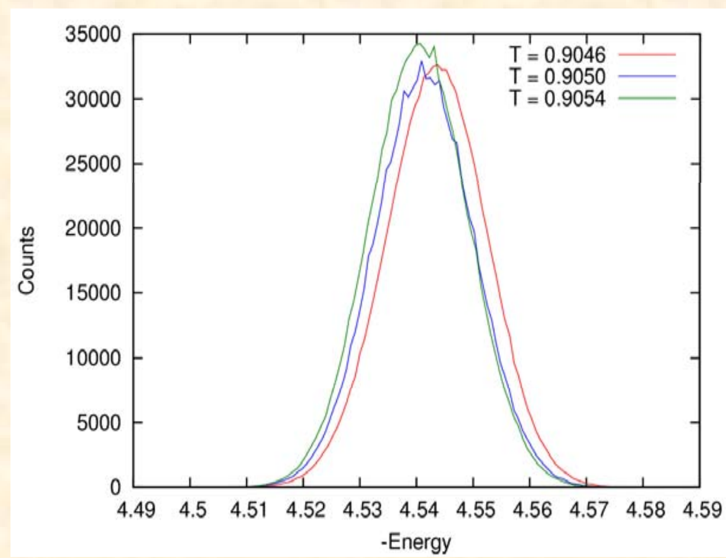

Energy histograms do not separate into 2 peaks near T_N for $K_{eff} > 0$

->Transition appears continuous,
as anisotropy removes continuous degeneracy

3D fcc Kagome Linear Spin Wave Theory

2D

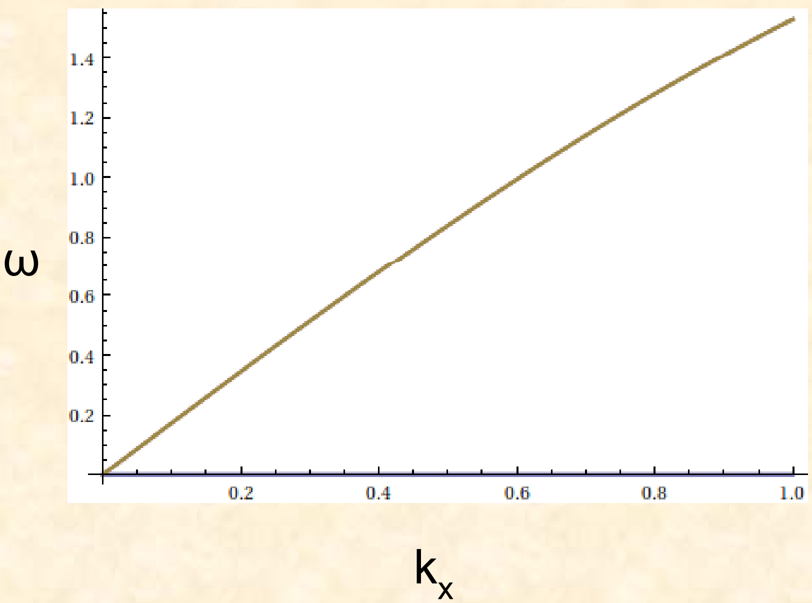

3D

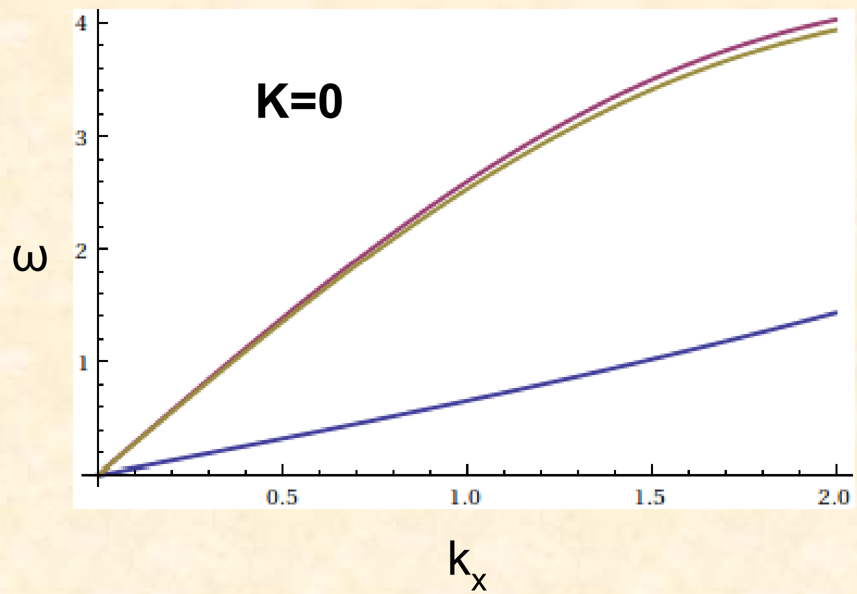

- 2 equal (yellow) states
- 1 ω = 0 (blue) state

- 3D lifts ω = 0 state and splits other states

-Efforts ongoing to add anisotropy to spin wave theory

Grain Size Progression vs. Areal Density

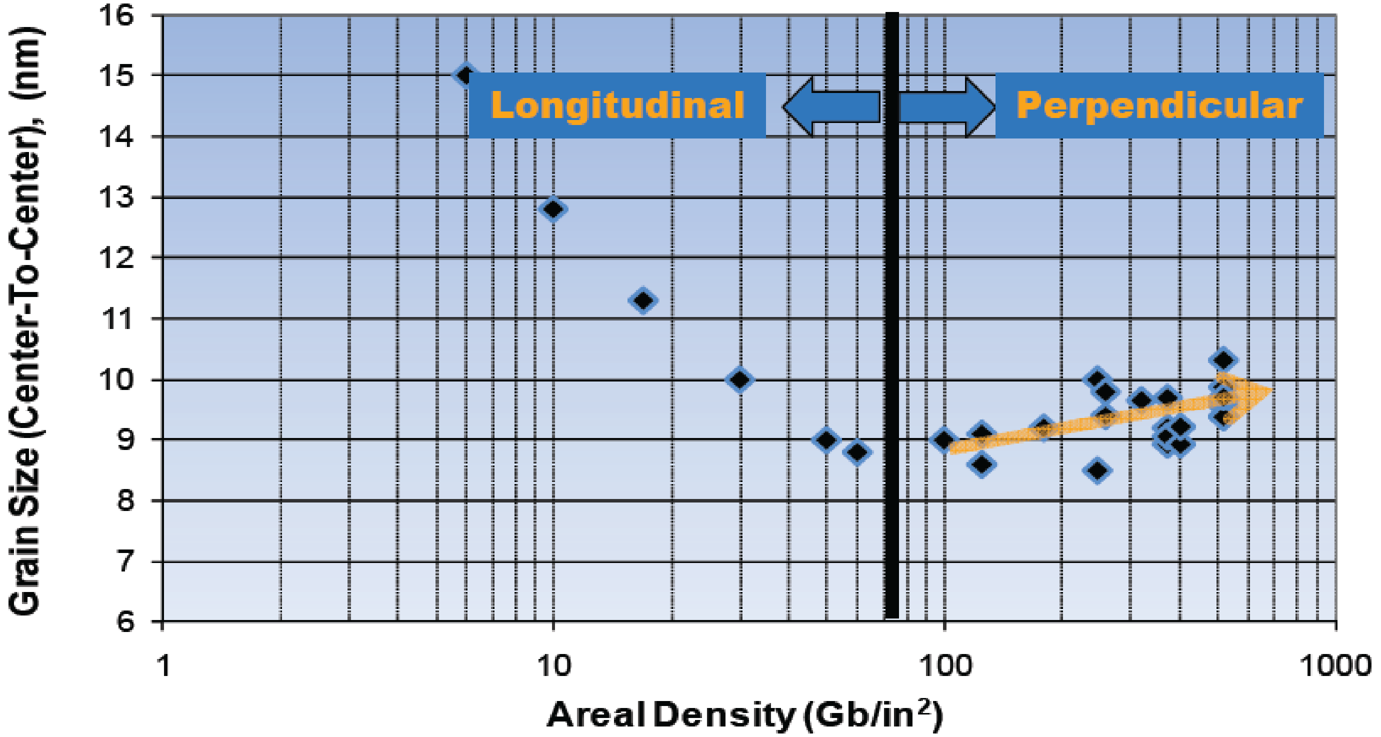

- ECC media structure was expected yield higher areal density capability by enabling smaller grain size in media.
- In practice, grain size has remained practically unchanged since PMR introduction.
- Instead, the trade-off of choice was to use ECC media to improve writability, maintain acceptable adjacent track erasure, and optimize transition parameter with utilization of higher Ku alloys and optimization of lateral exchange coupling through the various layers.

Monte Carlo simulations of the fcc Kagomé lattice.

Interlayer coupling J’.

J=1

Set inter-layer to J’ < 1.

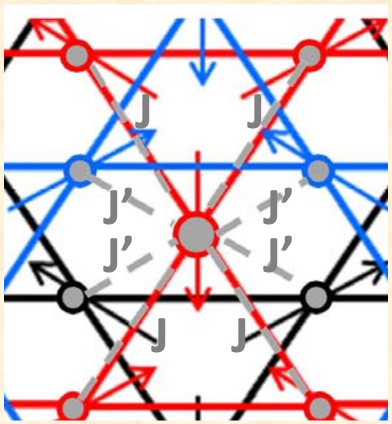

Specific Heat

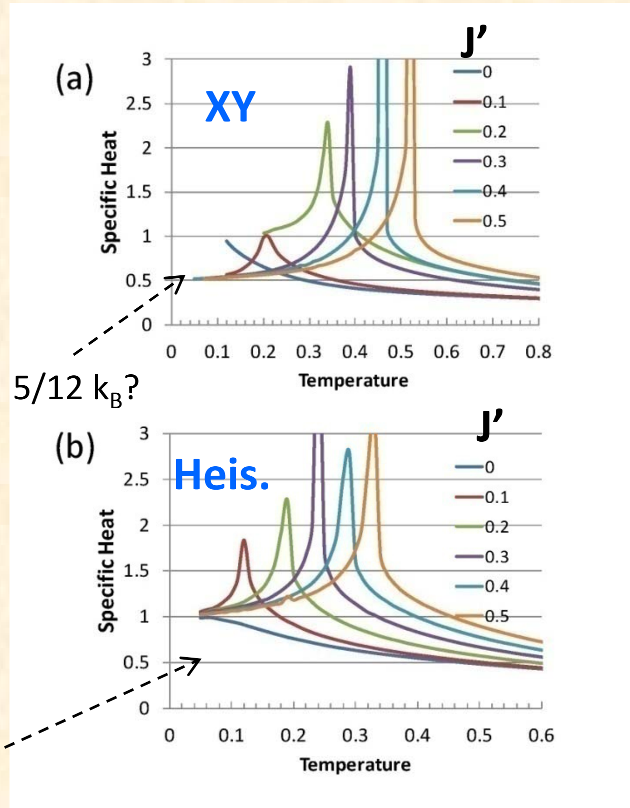

11/12 k_B?

T_N vs J’.

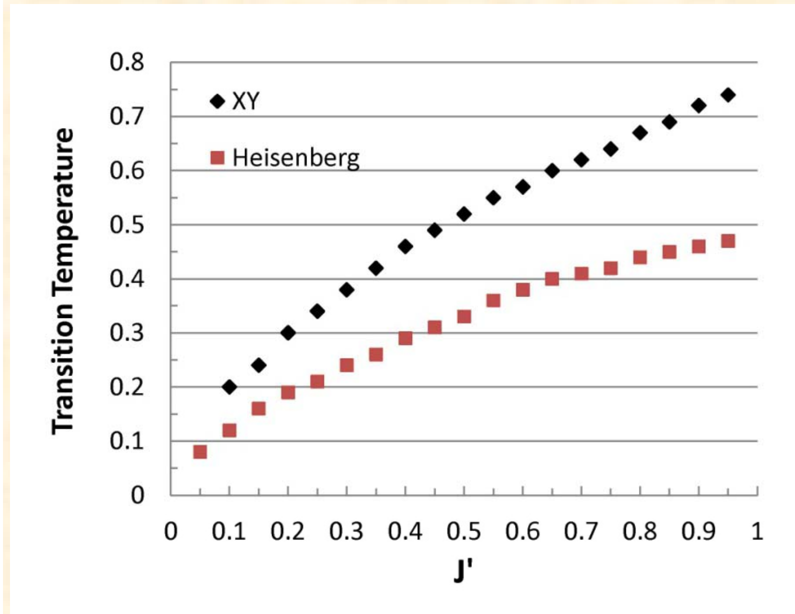

Trends are similar to other quasi 2D systems.

Monte Carlo simulations of the fcc Kagomé lattice.

V. HEMATTI, M.L. PLUMER, J.P. WHITEHEAD, Memorial University of Newfoundland,
B.W. SOUTHERN, University of Manitoba

http://www.mun.ca/physics/

http://www.physics.umanitoba.ca/

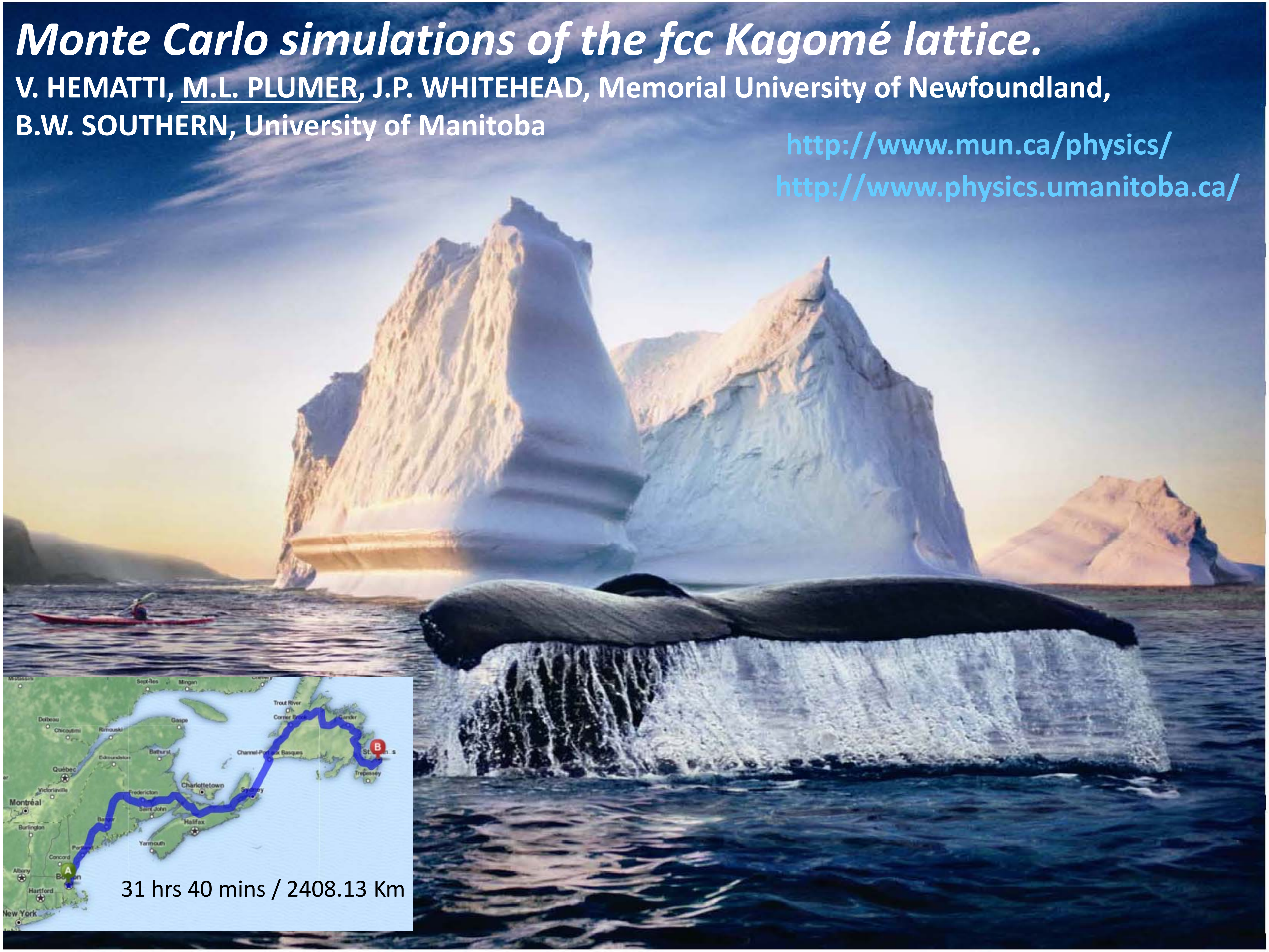

Finite Element Method: *Magsoft*

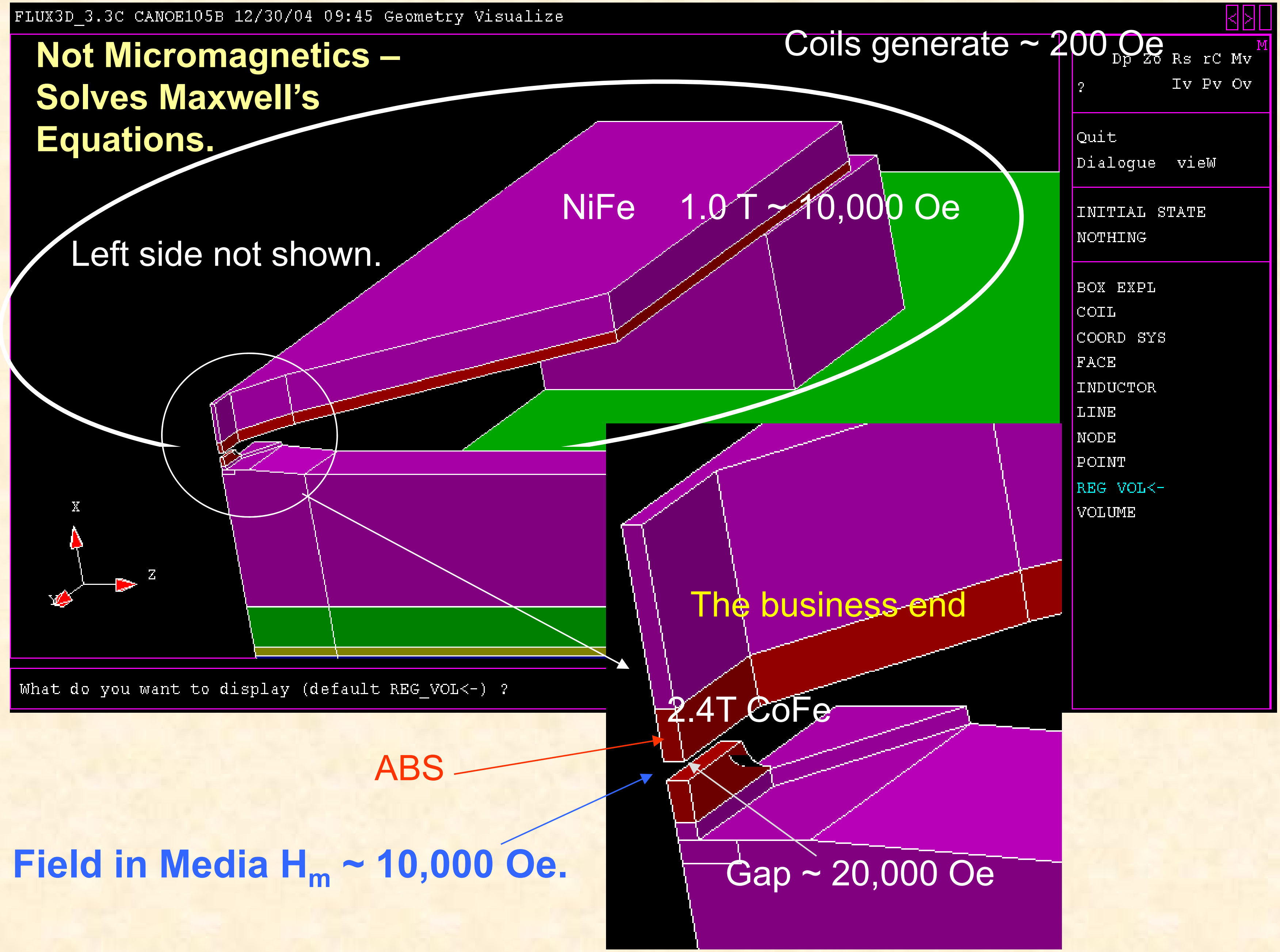

ABS

Field in Media H_m ~ 10,000 Oe.

X-section and ABS view of an Integrated MR Head

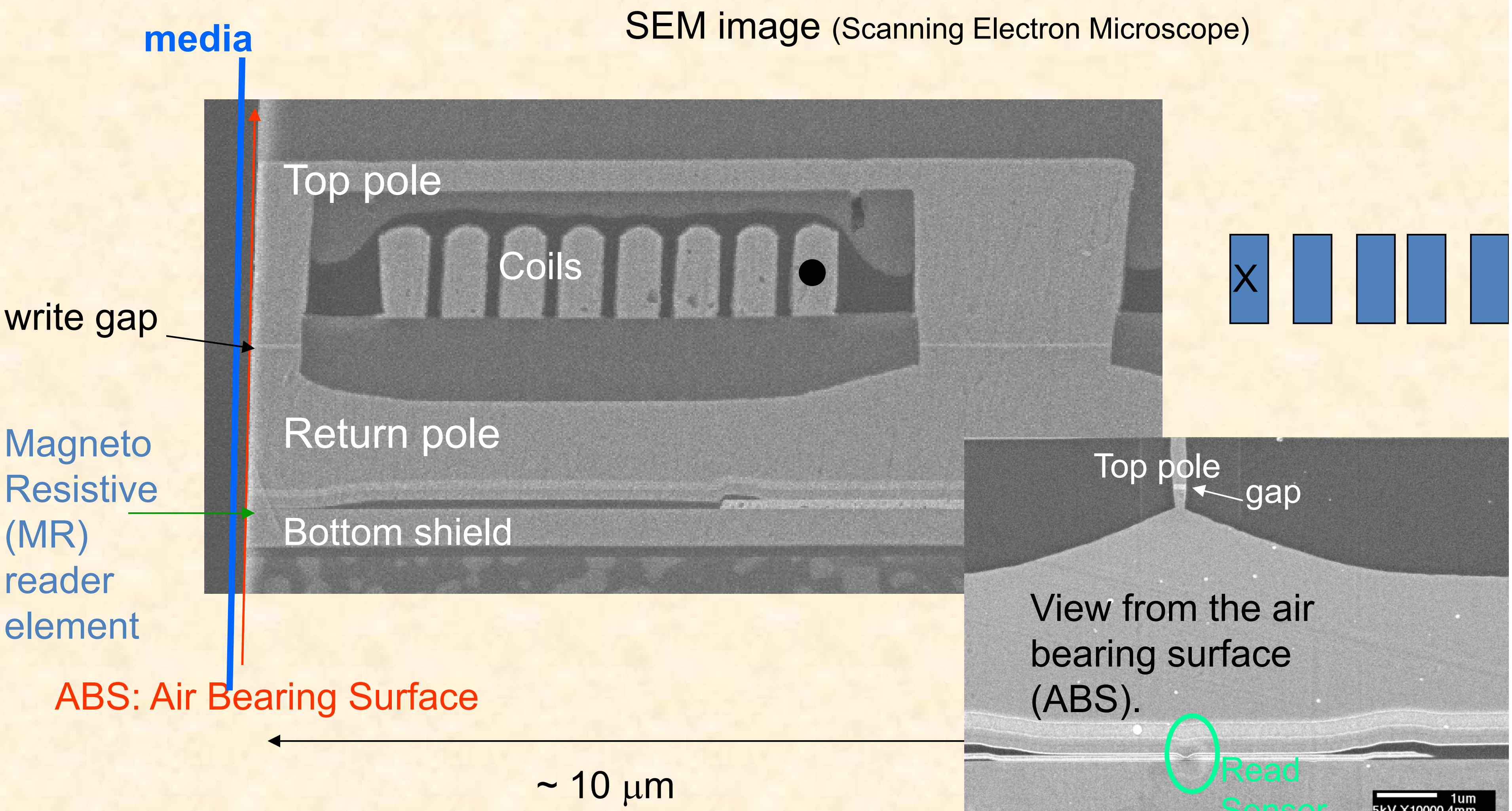

The Media: A model of granular recording media

Cobalt Atoms ⇒ Hexagonal Crystal Structure: *High Anisotropy*

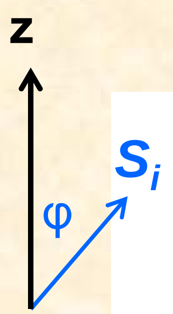

Energy = -K$cos^2\varphi$

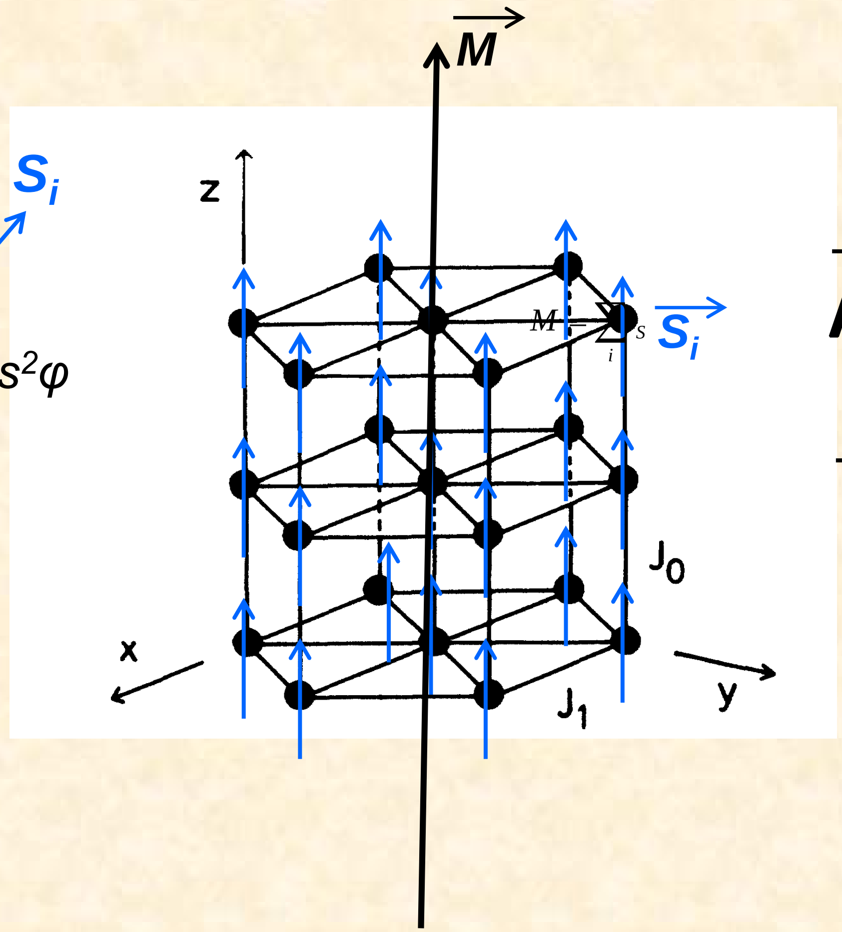

1000s of Atomic spins

$$\vec{M} = \sum_i \vec{S}_i$$

Total magnetization

Anisotropy

$\Rightarrow \vec{M} \parallel \hat{z}$

ABC stacked Kagomé

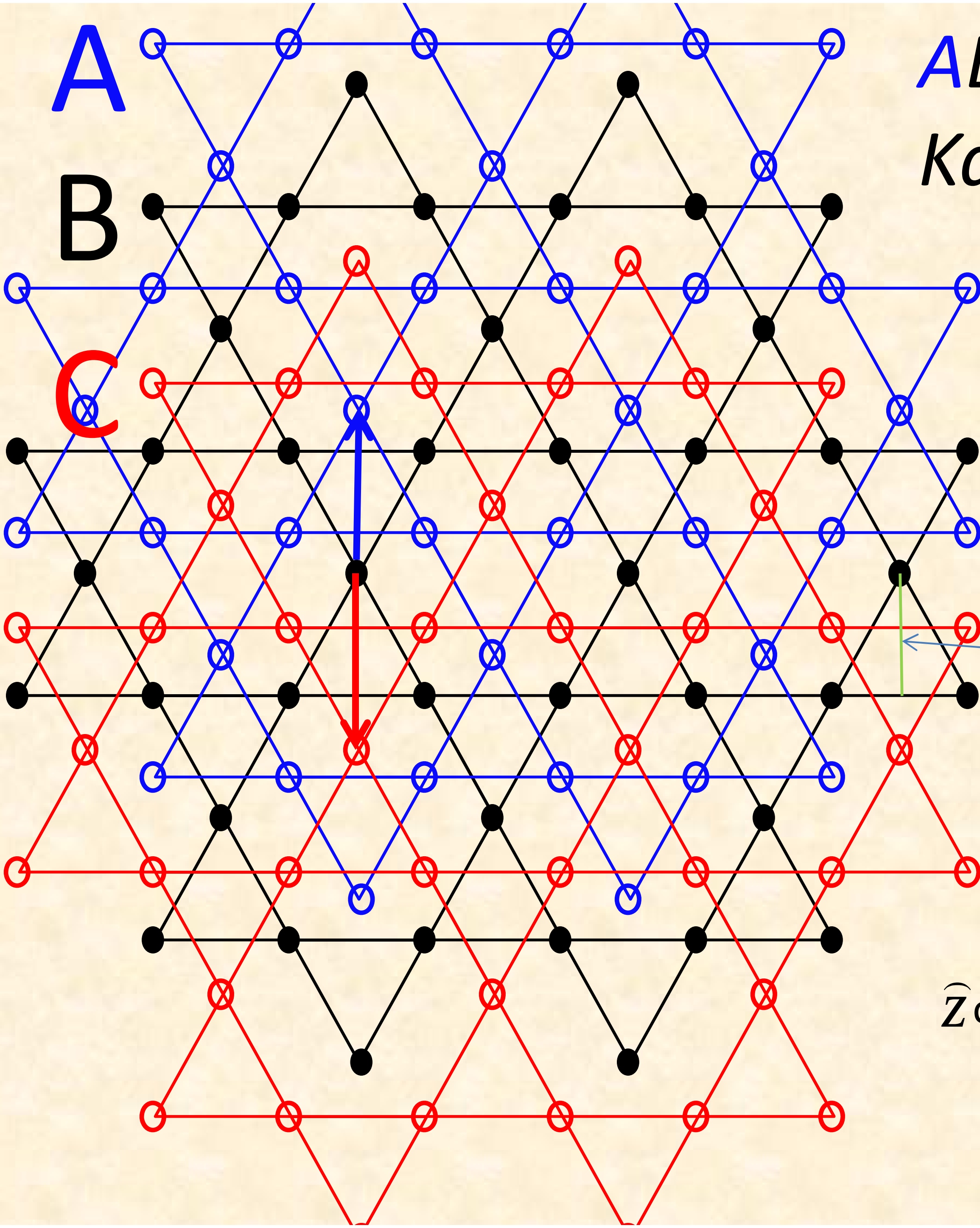

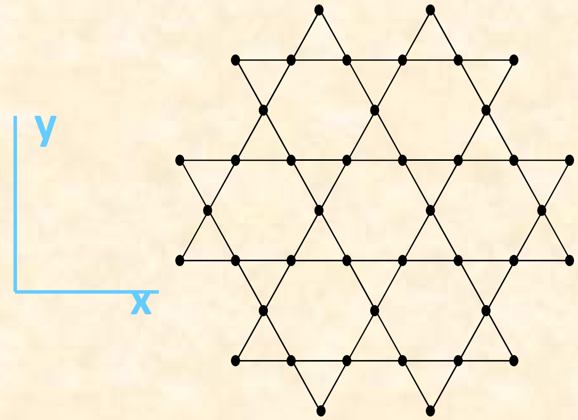

$b = (\sqrt{3}/2)a$

$w = \frac{4}{3} b\hat{y} + \frac{1}{3} c\hat{z}$

$w = -\frac{4}{3} b\hat{y} - \frac{1}{3} c\hat{z}$

$\hat{z}$ out of page, along <111>

Ferromagnets: Cannot ignore “magnetostatic” fields.

$$\vec{H}(\vec{r}) = -\int_V d\tau \frac{\vec{\nabla}\cdot\vec{M}(\vec{r}\,')(\vec{r}-\vec{r}\,')}{|\vec{r}-\vec{r}\,'|^3} + \int_S dA \frac{\hat{n}(\vec{r}\,')\cdot\vec{M}(\vec{r}\,')(\vec{r}-\vec{r}\,')}{|\vec{r}-\vec{r}\,'|^3}$$

Long range interaction ~ $1/r^3$

For grains of finite size, it’s not just dipole-dipole

Increases computational demands.

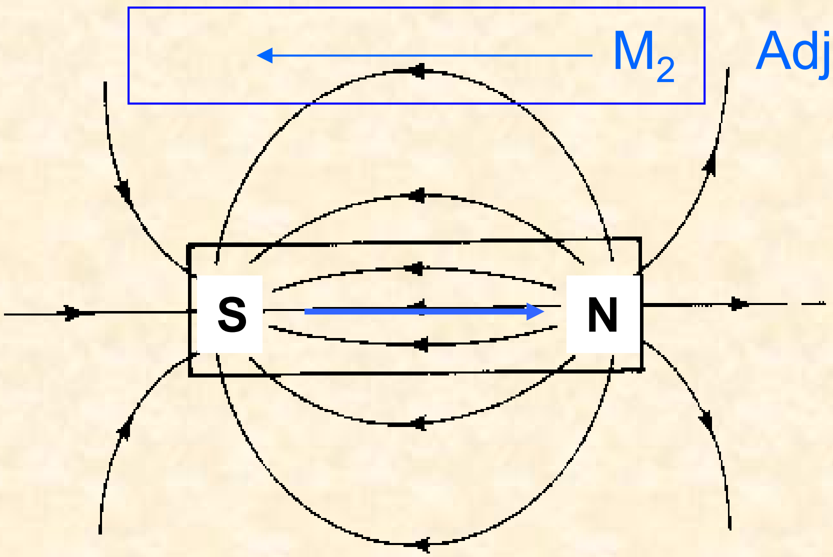

Adjacent bar magnet lies anti-parallel

- **Outside of bar M=0; H = B = stray field**
- **Inside of bar B = H + 4 π M_r, ‘demagnetizing’ field H opposes M**

H. Takahashi et al, J. Appl. Phys. 110, 123920 (2011)

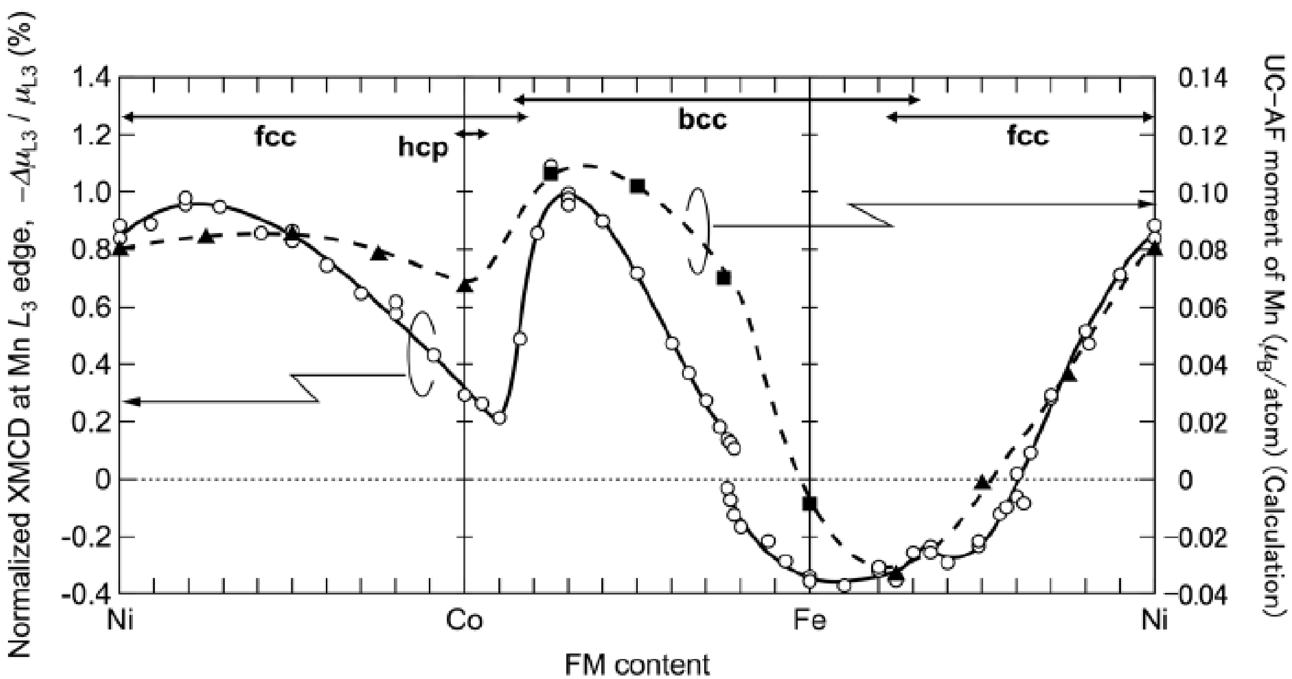

FIG. 8. Comparison of the experimental and calculation results for the net magnetic moments in the Mn-Ir/(Ni-Co, Co-Fe, Fe-Ni) bilayer system. The circle marks represent the experimental results. As the calculation results, the bcc structure (triangle marks) was employed for Co_3Fe_1, Co_2Fe_2, and Co_1Fe_3, Fe_4, and the fcc structure (square marks) was employed for the other compositions. This facilitated comparison with the results of the experimental analysis.

It comes in other forms…

Sakuma et al, JPSJ 69, 3072 (2000); PRB 67, 024420 (2003).

Relevant for sputtered thin films.

1. **Disordered $IrMn_3$: 3Q SDW**

Fishman et al, PRB 61, 12159 (2000).

2. **Disordered Ir_xMn_{100-x}: 2Q SDW**

DFT calculations

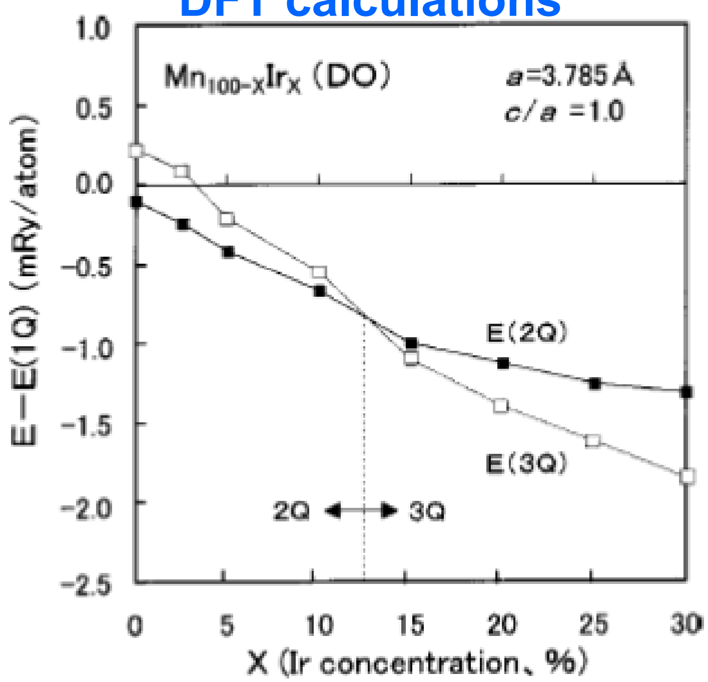

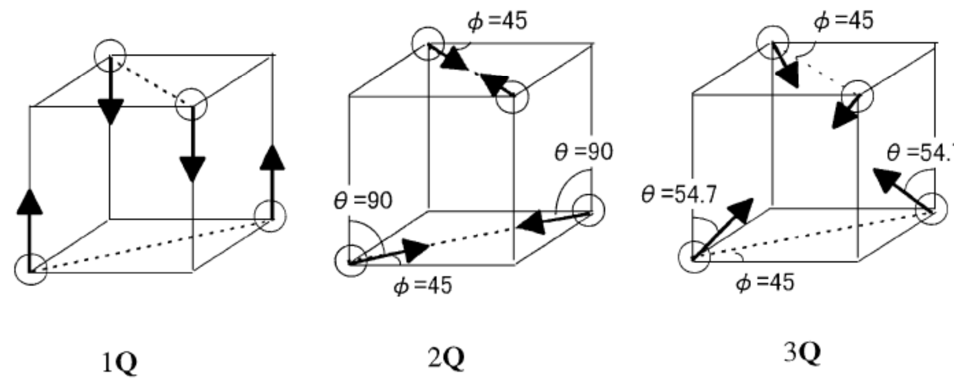

Fig. 1. Multiple-Q spin density wave structures in fcc lattice.